ASSESSMENT OF POTENTIAL EXPOSURE PATHWAYS IN KARST GROUNDWATER SYSTEMS IN NORTHERN PUERTO RICO USING GIS

by
KATHERINE M. STEELE VALENTÍN

A project submitted in partial fulfillment of the requirements for the degree of

MASTER in ENGINEERING
CIVIL ENGINEERING

UNIVERSITY OF PUERTO RICO
MAYAGÜEZ CAMPUS
2011

Approved by:

_____	_____
Ingrid Y. Padilla, PhD President, Graduate Committee	Date
_____	_____
Eric Harmsen, PhD Member, Graduate Committee	Date
_____	_____
Raul E. Zapata López, PhD Member, Graduate Committee	Date
_____	_____
Lysa Chizmadia, PhD Representative of Graduate Studies	Date
_____	_____
Ismael Pagán Trinidad, MSCE Chairperson of the Department	Date

Abstract

The North Coast Karst Aquifer System of Puerto Rico is the most productive aquifer of the island. Same characteristics that makes it highly productive, makes it vulnerable to contamination. This research assess potential path for contaminant exposure in Vega Alta-Dorado area using GIS. Groundwater velocity vectors were obtained and used for the developing of the longitudinal direction of the pathway. For the transversal direction dispersion was calculated with different dispersivity values, showing changes in the lateral extent. The results show that inside the pathway from Vega Alta Public Supply Well superfund site several wells with VOC were contained. The lateral extent of the contamination could not, however, be captured from average groundwater flow phenomena in the system. Results suggest greater dispersion, dynamic transport phenomena and/or the potential presence of other sources of contamination. GIS made it possible to visualize the extent of contamination and the potential points of exposure.

Resumen

El acuífero de la zona cársica del norte de Puerto Rico es el de mayor producción en la isla. Las mismas características que lo hacen tan productivo, también lo hace bien vulnerable a la contaminación. Esta investigación pretende estudiar las rutas potenciales de exposición de contaminantes en el área de Vega Alta-Dorado utilizando sistema de información geográficas (SIG). Se obtuvo la dirección del agua subterránea para el desarrollo de la dirección longitudinal de la ruta de contaminación. Para la dirección transversal se calculó la dispersión con distintas dispersividades, demostrando el cambio de la extensión lateral de la ruta. Los resultados demostraron que dentro de la ruta de contaminación desde el superfondo Vega Alta Public Supply Well se encontraban varios pozos con VOC. Sin embargo, varios pozos no se encontraban dentro de la ruta, lo que sugiere una mayor dispersión, transporte dinámico y/o otras posibles fuentes de contaminación. GIS hizo posible la visualización de la expansión de la contaminación y los posibles puntos de exposición.

Dedication

I want to dedicate this project to certain persons that help me emotionally through these years. First, to my husband, for all his support and love, for his patience and for believing in me from the day one when I told him that I wanted to get my master's degree. To my sons, Rommy and Ian, because their hugges and kisses made my day, even in the busiest ones. To my parents and sisters for all the cheers they have given to me. Finally, but not less important, this is a dedication to God, because without Him I will be nothing; He saved me and gave me the opportunity of finishing my master's degree. May His name be exalted, honored, and glorified.

Acknowledgements

Foremost, I will like to show my gratitude to my advisor Dr. Ingrid Y. Padilla for all the support and assistance given to me. Her motivation, enthusiasm, and knowledge were a great help on finishing this project. I will never forget that she believed in me on every phase during these years. Deepest gratitude are also due to the other members, past and present, of the graduate committee, Dr. Eric W. Harmsen, Dr. Raul E. Zapata and Dr. Jorge Rivera Santos, for accepting to be part of this project and for their insightful comments. Also, thanks to the chairman of the Civil Engineering and Surveying department, Prof. Ismael Pagán, for taking his time to read my project and for his comments.

It is very important for me to acknowledge the agencies that help me with the data collection: Environmental Protection Agency, US Geologic Survey, Puerto Rico Aqueduct and Sewer Authority, Puerto Rico Water Research Institute, Puerto Rico Planning Board and Environmental Quality Board. Also, I should thank the student Fransisco Torres, for sharing with me the first GIS data and for giving me the first tutorial on ArcGIS.

These years of study would have been very hard without the economic assistance that the Civil Engineering and Survey Department have given to me. Dr. Ingrid Y. Padilla and Dr. Didier Valdez gave me the opportunity to work at their side. Also, I'd like to mention the scholarship José Trio Monges, for funding me the opportunity to expose part of my work in international conference. It was a great opportunity and unforgettable experience.

Special thanks are given to all my family for their support, especially my husband, Nelson R. Gómez, for his proofreading and even his ideas. And last, but not least, a special thanks to God for giving me the strength through all these years.

Table of Content

List of Figures

List of Tables

1 Introduction

Karst groundwater systems develop in soluble rocks, such as limestone, and are characterized by high permeability and well-developed conduit porosity (Ford and Williams, 2007). These systems provide important freshwater resources for human consumption. The same characteristics that make karst aquifers highly productive make them highly vulnerable to contamination. As a result, karst aquifers could serve as an important route for contaminants exposure to humans and wildlife. The potential for exposure, as well as its magnitude and characteristics, depend on the source and nature of the contaminants; the physical, chemical and biological characteristics of the system; the fate and transport processes; the point and mode of exposure; and the receptor population (ATSDR, n.d.). Contaminated sites overlaying karst systems constitute important sources of contamination. These include superfund sites, landfills, and areas impacted by toxic releases. Once released into the groundwater, contaminants are transported to potential exposure sites, where humans may become in contact.

Water quality surveys in Puerto Rico have shown a vast area of contamination of the northern karst aquifer of Puerto Rico (Guzmán-Ríos, et al., 1986; USGS, 2008). Of great concern has been the contamination of chlorinated chemicals and phthalates because of their adverse health impacts (Padilla and Steele, 2008). These contaminants have been associated with decreased gestation length (Latini, et al., 2003), reproductive and neurological damage, increased birth defects, decreased birth weight, increased risk for spontaneous abortion, and pre-term birth among others. Puerto Rico has the highest rate of pre-term rate in United States (March of Dimes, 2007). The known factors for prematurity (e.g., late prenatal care, tobacco use) however, do not explain the increase in these rates (March of Dimes, 2007).

The overall objective of this project is to assess potential contaminant exposure paths in the karst groundwater system of northern Puerto Rico using geographic information systems (GIS) technologies. It further aims to develop improved methods for predicting human exposure through karst aquifer using GIS technologies. The project focuses in potential path for exposure of chlorinated organic chemicals in the Vega Alta-Dorado area, part of La Plata-Arecibo hydrological system.

2 Literature Review

Karst terrains are underlain by soluble rocks, primarily limestone and dolomite, which undergoes considerable dissolution along joints, fractures, bedding planes, and other openings in which groundwater flows (Ford and Williams, 2007). These terrains show distinctive surface and subsurface features associated with sinkholes, springs, caves, sinking, losing, and gaining streams. Subsurface environments in karst terrains are characterized by well-developed conduit porosity and highly transmissivity zones (Leibundgut, et al., 1998). These characteristics make groundwater systems in karst areas highly productive and important freshwater resources for human consumption and ecological integrity of streams, wetlands, and coastal zones. Karst areas occupy large areas of the planet's ice-free continental areas (~20%) and provide roughly 20-25% of the global population water needs (Ford and Williams, 2007).

In Puerto Rico, karst areas cover over 17% of the island (Veve and Taggart, 1996). The north coast karst aquifer is the most productive aquifer of the island (Veve and Taggart, 1996), serving as a significant source of drinking water and supporting important ecosystems. During 1990, groundwater provided over 60% of the water supplied to the region for public, industrial, and agricultural uses (Molina-Rivera, 1996a; Molina-Rivera, 1996b). The municipality of Arecibo, in the North Coast karst belt, extracted the largest amount of ground in the entire island (Molina-Rivera, 1996b).)

The same characteristics that make karst groundwater system highly productive, makes them highly vulnerable to contamination (Göppert and Goldscheider, 2008), and impart an enormous capacity to store and convey contaminants from sources to potential exposures zones. As a result, karst aquifers could serve as an important route for contaminants exposure to humans and wildlife. Water quality surveys in Puerto Rico have shown a vast area of contamination of the northern karst aquifer (Guzmán-Ríos, et al., 1986). Of great concern has been the contamination with chlorinated chemicals, which have been measured in a large percentage of sample wells (USGS, 2008; Sepúlveda, 1999). Extensive contamination has resulted in the closure of 41% of drinking water supply wells in the north coast aquifer by 1987 (Zack, et al., 1987). Since then, there have been more closures. Among heavily affected physiographical areas is the La Plata-

Arecibo hydrological system in northern Puerto Rico, which extends between Rio La Plata and Rio Grande de Arecibo watersheds. Included in this region, the municipalities of Arecibo, Barceloneta, Vega Baja, Vega Alta, and Toa Baja have been affected by a long history of toxic spills and chemical waste and industrial solvent release into the subsurface (Zack, et al., 1987; Hunter and Arbona, 1995) (Figure 2-1 and Figure 2-2). The municipalities in the La Plata-Arecibo region are coincidentally among the areas with highest groundwater extraction (Molina-Rivera, 1996b). Groundwater discharge from this system to streams, wetlands, and coastal areas is also an important component of the region's ecosystems.

Long and extensive history of contamination, high vulnerability for further contamination, and high potential for exposure makes the La Plata-Arecibo hydrological system region ideal for assessment of potential exposure, related adverse impacts, and effective strategies to reduce exposure and potential public health and the environment in the northern karst region of Puerto Rico. This section presents a description of: the study area and its primary potential sources of contamination; contaminant exposure pathways; potential adverse health impacts of targeted contaminants; and previous studies applying GIS technologies for risk assessment of contamination.

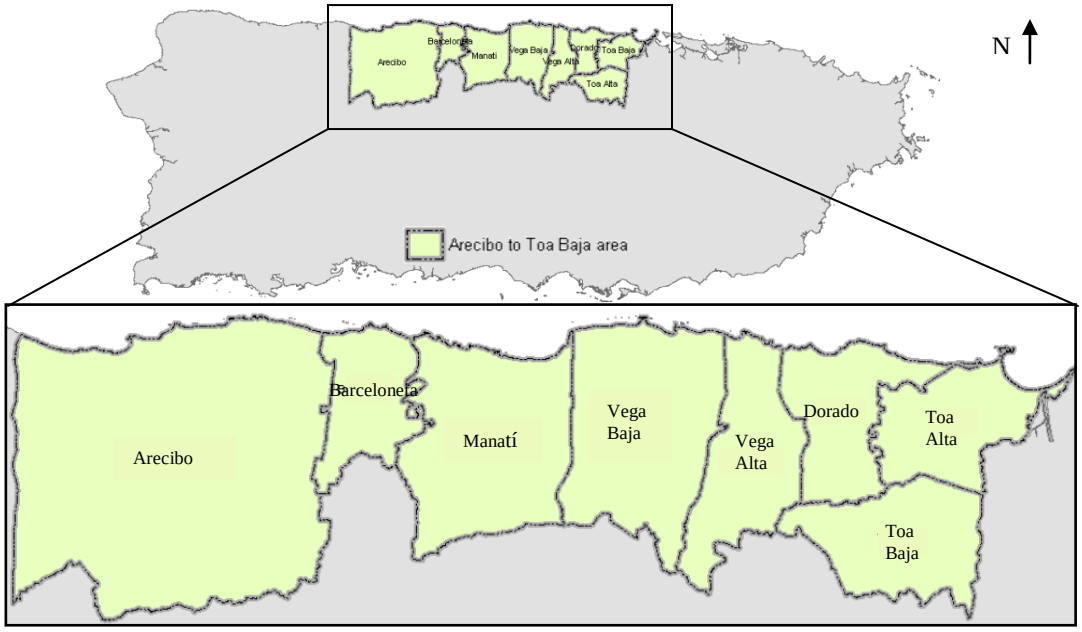

Figure 2-1 La Plata-Arecibo study area in northern Puerto Rico (Source: PRWRERI 2007)

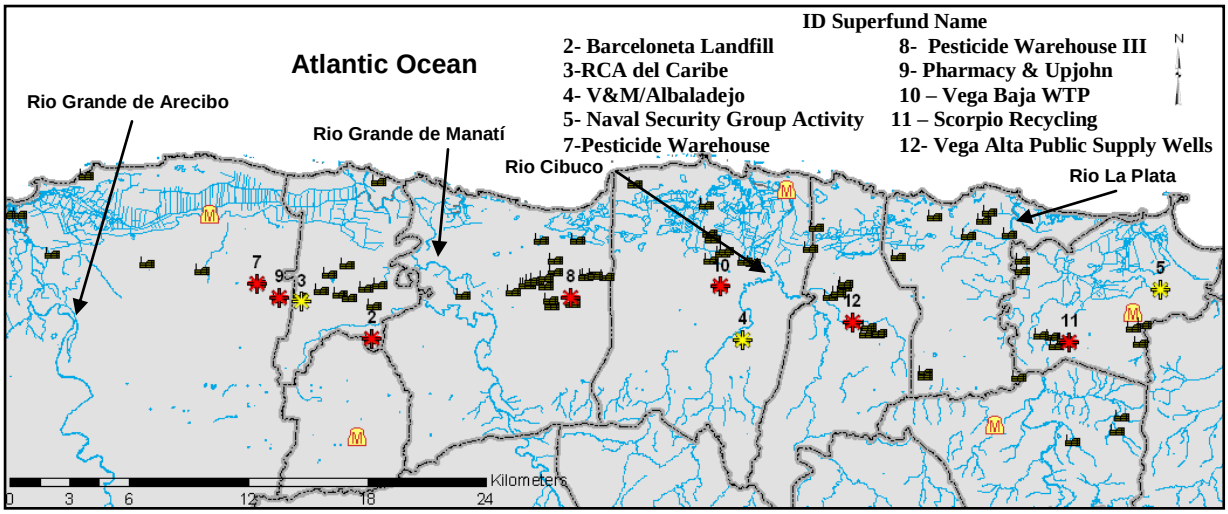

(b)

Inactive Superfund | Active Superfund | Toxic Release Inventory Site | Landfill | Hydrology

Figure 2-2: La Plata-Arecibo study area in northern Puerto Rico (a) and associated potential contamination sources (b).

Long and extensive history of contamination, high vulnerability for further contamination, and high potential for exposure makes the La Plata-Arecibo hydrological system region ideal for assessment of potential exposure, related adverse impacts, and effective strategies to reduce exposure and potential public health and the environment in the northern karst region of Puerto Rico. This section presents a description of: the study area and its primary potential sources of contamination; contaminant exposure pathways; potential adverse health impacts of targeted contaminants; and previous studies applying GIS technologies for risk assessment of contamination.

2.1 La Plata – Arecibo Study Area

The La Plata – Arecibo study area comprises an area extending from Río La Plata watershed, on the east, to the Río Grande de Arecibo watershed on the west (Figure 2-2). On the north, the area is bound by the Atlantic Ocean and on the South it is limited to the extent of the limestone outcrop (Figure 2-3). La Plata – Arecibo region is transverse by four major rivers (Río Grande de Arecibo, Río Grande de Manatí, Río Cibuco, and Río La Plata) and it is overlain by the North Coast Limestone Aquifer System.

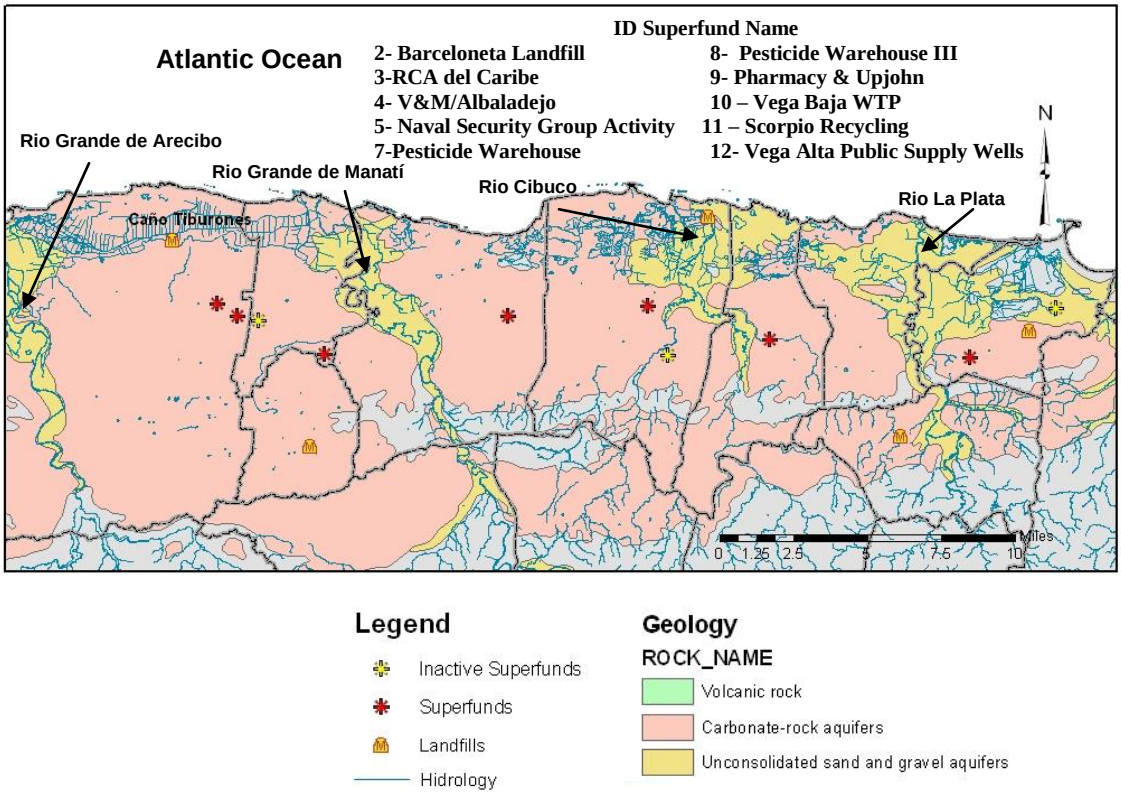

Figure 2-3: Surficial geology of study area

The North Coast Aquifer System consists of three units: upper, middle and lower (Veve and Taggart, 1996). The upper unit is the unconfined aquifer, the middle unit is the confining unit, and the lower unit is the confined aquifer (Figure 2-4). The lower confined unit is vulnerable to contaminants only on outcrops areas. To the north of the outcrop, it is generally less vulnerable for potential contamination because of the higher depth of the aquifer and poor connection to surface features (streams, wetlands, springs). The upper aquifer is vulnerable to contamination over the entire area, and can provide several routes of potential exposure to contaminants. This aquifer extends from the surface to a depth of up to 1,075 ft below surface (Rodríguez-Martínez, 1994). It is physically accessible for groundwater extractions. In year 2004 this aquifer provided 52% of water production in Puerto Rico's north-central area (DRNA, 2008). Also, it is hydraulically connected to surface features which can serve as potential exposure routes. This project focuses on the upper limestone aquifer of the La Plata-Arecibo region.

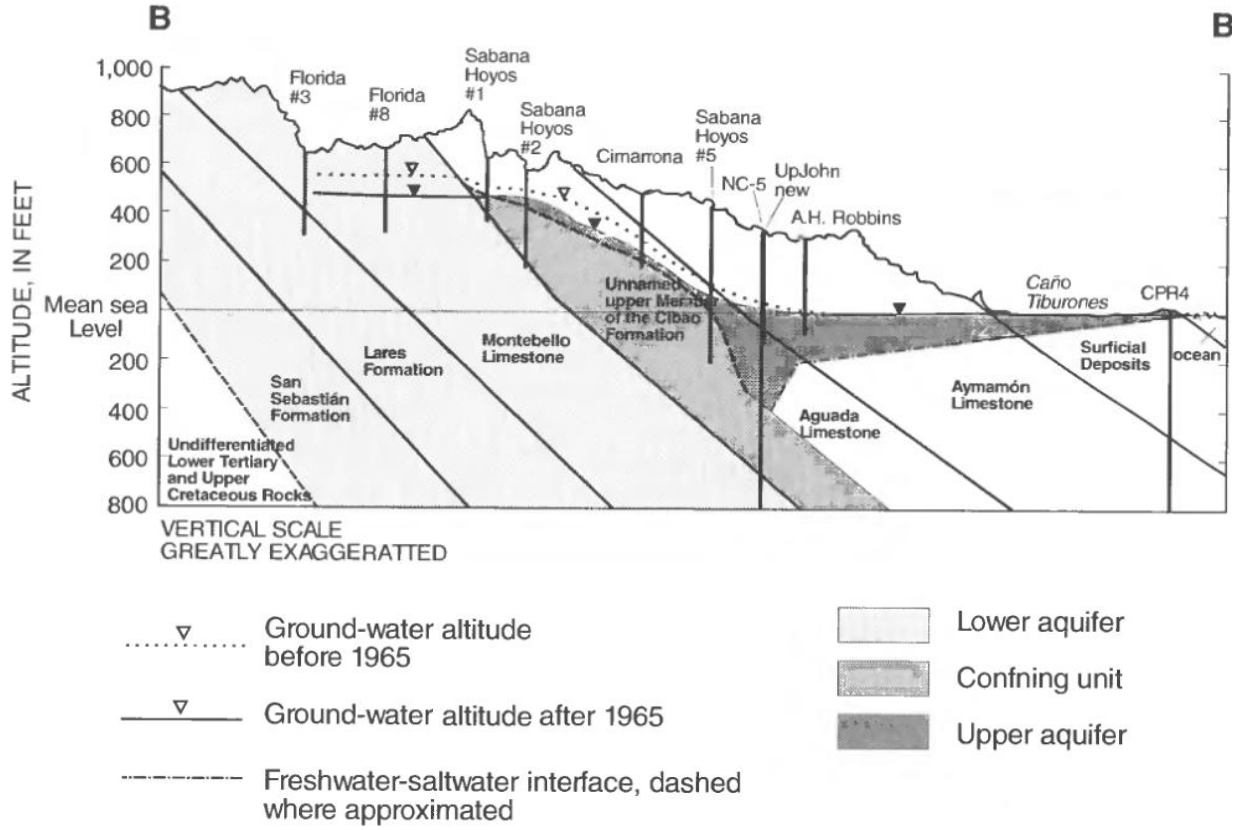

Figure 2-4 Cross-section of the North Coast Aquifer System (Source: Torres-González, 1996)

The highly permeable Aymamón and Aguada Limestone make up the upper aquifer (Renken, et al., 2002). These hydrogeologic units range from chalky beds on the bottom of the Aguada to pure limestone at the top of the Aymamon (Monroe, 1980), and show highly variable porosity and permeability properties. High permeability contrast in short distances reflects the variable distribution of conduit porosity. Groundwater enters the system through surface infiltration and direct injection of runoff into karstic conduits (e.g., sinkholes). Generally, water in the aquifer flows northward toward the Atlantic Ocean and toward streams. Discharge is principally to wells, coastal wetlands, springs, and streams (Renken, et al., 2002).

The climate in the La Plata-Arecibo region is tropical marine, mild with little seasonal variations in temperature averaging about 25.5°C and an evapotranspiration rate of about 45 inches per year (Giusti and Bernett, 1976; Cherry, 2001; DRNA 2005). It is characterized by two wet seasons and one dry season. Generally, wet periods occur between April and May and from

July through November. Dry periods occur mostly from December through March. Average annual rainfall in the area is about 60 inches near the coast to 70 inches in the karst terrain near the southern boundary of the aquifer (Cherry, 2001).

The La Plata-Arecibo area houses a total population of 459,732 (Census Bureau, 2000). The area contains a wide range of land uses including residential, industrial, and agricultural activities, and natural reserves.

2.1.1 Contamination Sources

Water and soil quality surveys (Guzmán-Ríos et al., 1986; USGS, 2008; EPA, 2008a) have shown vast contamination in the La Plata-Arecibo study area. Sources of this contamination include superfund sites, landfills, dry cleaners, pharmaceutical industries, and other sites impacted by toxic release (EPA, 2010c).

Serious contamination has prompted inclusion in the National Priority List (NPL) of 10 sites within La Plata-Arecibo hydrogeological region (Figure 2-2 and Table 2-1). The NPL is the list of national priorities among the known releases or threatened releases of hazardous substances, pollutants, or contaminants throughout the United States and its territories. This list includes heavily-contaminated sites with high potential risk of exposure that have been designated as high priority for clean up. According to the Environmental Protection Agency (EPA) superfund website, many heavily-contaminated sites exists that have not been listed in the NPL. Seven of the 10 sites within La Plata-Arecibo area are still active, but the others could have contributed to contamination at the system level.

Five of these sites (Barceloneta Landfill, Scorpio Recycling, Upjohn, Vega Alta Public Supply Wells, and the Vega Baja Landfill) have been contaminated with chlorinated solvents, including: TCE, Dichloroethene (DCE), Chloroform, Carbon tetrachloride, tetrachloroethene (PCE), tetrachloroethane (TCA), dichloroethane (DCA), and methylene chloride (MC). Four of the sites (Pesticide Warehouse III, Scorpio Recycling, Vega Baja Landfill, and the Barceloneta Landfill) have reported phthalate contamination, mostly with Dibutyl phthalate (DBP) and Di(2-ethylhexyl) phthalate (DEHP) (EPA, 1987a; EPA, 1988; EPA, 1996; EPA, 2004; ATSDR 2005; EPA 2006a; EPA, 2008c). Recently, the EPA issued orders to close landfills in Toa Baja,

Florida, Vega Baja, Aguadilla, and Santa Isabel, due mainly to substantial concern of the drinking water quality associated with the landfills (EPA, 2006b). In the northern area of PR, these landfills are unlined and located on karst areas where pollutants can get directly to the ground water.

Table 2-1: NPL Sites in La Plata-Arecibo Region

ID	City	Site Name	Proposed Listing	Final Listing	Contaminant	Media
7	Arecibo	Pesticide Warehouse I	09/23/04	09/27/06	Pesticides	Soil, GW
9	Arecibo	Upjohn Facility	09/08/83	09/21/84	VOC	GW
2	Barceloneta	Barceloneta Landfill	12/30/82	09/08/83	Metals, VOC	GW
8	Manatí	Pesticide Warehouse III	09/05/02	04/30/03	Pesticides, Metals	GW, Soil
10	Vega Baja	Vega Baja WTP	04/23/99	07/22/99	Metals, VOC	GW
12	Vega Alta	Vega Alta Public Supply Wells	09/08/83	09/21/84	VOC	GW
11	Toa Baja	Scorpio Recycling	10/22/99	02/04/00	Metals, VOC	GW
3	Barceloneta	RCA del Caribe	12/01/82	9/01/83	Ferric Chloride	Water
4	Vega Baja	V&M/Albaladejo	06/17/96	12/23/96	Metals	Soil
5	Toa Baja	Naval Security Group	06/24/88	10/04/89	Metals, Pesticides	Soil

* ID = ID superfund name from Figure 2-1
* VOC = volatile organic compound
* Superfund ID 3, 4 and 5 are inactive

Landfills are very complex systems where various biogeochemical interactive processes occur simultaneously. Most landfills contain phthalates-containing materials (PAMs), including plastics, food packaging, home furnishings, paints, clothing, medical devices, and cosmetic products (NIH, 2006). PAMs can degrade and serve as a potential source of phthalate contamination for groundwater. Indeed, phthalates have been commonly found in landfill leachates, including many listed in the NPL (ATSDR, n.d.; Bauer and Hermann, 1998; Randal, et al., 1994).

2.2 Solute Transport in Karst Groundwater Systems

Organic contaminants move through the karst aquifers by complex pathways, having the potential to store and transport significant contaminant mass for long periods of times (Loop and White, 2001; NRC, 2005). Transport of contaminants in karst ground-water system is highly influenced by the flow mechanism predominating in the aquifer. Conduit-flow dominated systems tend to convey solutes rapidly through the system without much attenuation. Diffuse-flow systems can significantly retard the movement of and store large quantities of contaminants, causing a long-term release of contaminant to the environment. Combined conduit- and diffuse-flow transport mechanism occur, over a wide range of hydrogeologic systems and flow conditions (Schilling and Helmers, 2008; White, 2002), but can be highly associated with karst systems with high matrix permeability, such as those found in carbonate aquifers of Puerto Rico (White, 2002). The upper aquifer of the north coast is characterized by both diffuse and conduit flow (Renken, et al., 2002). In such systems, conduits can concentrate water and contaminants from direct sources and/or diffuse flow and convey them rapidly to potential-exposure discharge points (e.g., springs). They can also convey contaminants to "trapping" diffuse-flow zones of greater contaminant storage capacity, where they can serve as a long-term source of contamination. Furthermore, discharge and potential exposures area in these types of systems are not limited to a particular point of discharge, but can potentially act as a diffuse source and potential exposure path over large discharge zones. Consequently, karst aquifers are among the most challenging hydrogeologic settings to characterize and manage (NRC, 2005).

The principal solute transport mechanisms are advection, diffusion, dispersion, sorption, and degradation (Delleur, 1999). Advection is the transport of a solute by the bulk groundwater flow (Delleur, 1999). Basically, it moves with the groundwater flow and follows its direction. In equivalent porous media, groundwater flow is described by Darcy's Law, which state that ground water flux (q) depends on the hydraulic conductivity of the media (K) and the hydraulic gradient (dh/dl) which is the change in hydraulic head (dh) over the change of distance (dl) between two points,

$$q = -K\frac{dh}{dl} \quad \textbf{(1)}$$

where;

q = Darcy velocity (ft/d)

K = Hydraulic conductivity (ft/d)

dh/dl = Hydraulic gradient

Flow direction for an isotropic system is estimated from hydraulic gradients. Advection processes are assumed in this work to be described by velocity vectors, which for equivalent porous media can be estimated from Darcy's velocity:

$$v = \frac{q}{n_e} \quad \textbf{(2)}$$

where;

v = Average interstitial velocity (average linear velocity) (ft/d)

q = Darcy velocity (ft/d)

n_e = effective porosity.

Groundwater flow in karst systems has been approximated to equivalent porous media in several large-scale (i.e. regional scale) models for water resources exploration (Cherry, 2001 and Torres-González, 1996). At smaller scales, conduit flow may dominate the flow and transport characteristics, and Darcy's law may not be applicable (Field, 1999). The work presented in this document assumes regional-scale flow and an equivalent porous media. Deviations from expected results may arise from this assumption.

Dispersion is the spreading of the plume that occurs along and across the main flow direction due to aquifer heterogeneities (Delleur, 1999). The study of dispersion phenomena involves the application of probability theory for predicting the spatial distribution of tracer particles with time in a porous media (Batu, 2006). The distribution of contamination in the plume is assumed to follow a Gaussian distribution for ideal homogeneous equivalent porous media. Thus, the

extension of the plume under these conditions can be represented with the standard deviation of the distribution (Fetter, 1999). The standard deviation of a Gaussian concentration distribution along the advective path is generally described as a function of travel time (t) and the hydrodynamic dispersion coefficient (D) (Fetter, 1999):

$$\sigma_x = \sqrt{2D_T t} \quad \textbf{(3)}$$

Dispersion transport occurs along (longitudinal dispersion) and across (transverse dispersion) the main direction of flow and it is often assumed to be function of the advective velocity (Fetter, 1999):

$$D_L = \sigma_L v_i + D^* \quad \textbf{(4)}$$

$$D_T = \sigma_T v_i + D^* \quad \textbf{(5)}$$

where;

D_L = Hydrodynamic dispersion of the coefficient parallel to the principal direction of flow (longitudinal) (ft^2/d)

D_T = Hydrodynamic dispersion of the coefficient perpendicular to the principal direction of flow (transverse) (ft^2/d)

σ_L = Longitudinal dynamic dispersivity (ft)

σ_T = Transverse dynamic dispersivity (ft)

v_i = Average linear velocity (ft/d)

D^* = Molecular diffusion.

Dispersivity is a parameter that is influenced by grain size, non-uniformity, grain form, pore size distribution and structural features (Hurst, 1991). This value varies depending on the aquifers material, but it is not derived from other basic properties, nor directly measurable. Work has shown that dispersivity varies with distance (Fetter, 1999; GSC et al., 1984; Delleur, 1999). Gelhar et al. (1979) showed that dispersivity tends to increase with distance, and derived a

function to obtain longitudinal dispersivity as a distance dependent coefficient. The function is given by:

$$\boldsymbol{\alpha_L = 0.1L} \tag{6}$$

Where;

α_L= longitudinal dispersivity (ft)

L = length of the flow path (ft)

Transversal dispersivity is assumed typically to be 1/10 to 1/100 of the longitudinal dispersivity (Delleur, 1999). The spatial relation of longitudinal and transversal disperivity is assumed to follow similar trends, although their magnitude is not known for karst aquifers.

Dispersivity is often assumed for modeling purposes, and even used as a calibration parameter (GSC et al., 1984). Because of the uncertainty on this parameter, it is important to analyze how the solution derived from the model would change (if at all) if the value assigned to the parameter were changed to other plausible values (Hiller and Lieberman, 2001). A sensitivity analysis studies the uncertainty of a model output changing values of a parameter in the model input (Saltelli et al., 2004).

Because of the large heterogeneities, anisotropy, and possible turbulent flow, dispersion terms in karst aquifers may be expected higher than those found in equivalent porous media. Concentration distributions may also show multiple-peak breakthroughs, indicating multiple flow paths (Goldscheider and Drew, 2007), and deviation from the Gaussian distribution. It is assumed in this study that dispersion can be described with a Gaussian distribution at the regional scale based on the assumption that the aquifer is a homogeneous equivalent porous media.

2.3 Contaminant Exposure Pathways

Contaminants released into karst groundwater systems move through complex pathways from their sources to discharge areas of potential exposure. Exposure of contaminated water can occur through ingestion, inhalation (in case of volatile contaminants), or dermal adsorption (Vrijheid,

2000). Ingestion exposure may occur from drinking water, as well as eating contaminated food (e.g., fish, vegetation, cattle). Points of exposure for drinking water include water wells, springs, and surface water sources with limited treatment (e.g., rural communities not served by the Puerto Rico Aqueduct and Sewage Authority). Contaminated water discharged to zones of agricultural activities, fishing, and recreation (i.e. Riparian zones, wetlands, coastal zones) may bio-concentrate in eatable goods and absorb through the skin.

In karst aquifers, exposure pathways are very complex. The interaction and relative flow rates of water and solutes in conduits and the rock matrix in karst aquifers lead to complex flow-dependent transport behavior (Loop and White, 2001). During times of rapid ground-water recharge, pressure heads increase in conduits and water and solutes flows rapidly through the conduit and enter adjacent pores and fissures (White, 1999). As pressure heads become lower during base flow, contaminants stored in fractures and rock matrix migrate through diffuse transport into the conduit, providing a long-term source of contaminants. Contaminants entering the system are subjected to multiple events of rapid mobilization during conduit storm flow followed by slower diffuse flow during baseflow conditions (Padilla and Steele, 2008). Over time, variable flow regimes cause significant dispersion of contaminants in the aquifer, extending the zones of potential exposure.

2.4 Relation of Contaminated Water and Health Effects

Chlorinated solvents are the contaminants of concern in this project because of their adverse effect in the environment, presence in listed and potential superfund sites in Puerto Rico, and potential for exposure and health impacts. Exposure to TCE has been related to several adverse health effects, including cardiac, neurological, hepatic, renal, dermal, immunological, and reproductive effects, increased birth defects, perinatal mortality, and cancer, and decreased birth weights (ATSDR, 1997). They are considered endocrine disruptors and carcinogens. Some epidemiologic studies of women exposed occupationally to TCE and other solvents have reported increased risk for spontaneous abortion and lower birth weight (Lipscomb and Fenster, 1991; Khattak, 1999; Ha et. al., 2002).

2.5 Use of GIS to Define Exposure Pathways

Geographic information systems (GIS) are used for capturing, organizing, storing, editing, analyzing, and managing geographically-referenced information. It permits integration of multiple set of spatially-related data. GIS can be used in groundwater for: mapping information such as water table depths, aquifer type and material, and aquifer recharge; managing site inventory data; computing statistics to estimate spatial correlation of a process occurring over a region such as nonpoint source pollution; estimating vulnerability of groundwater to pollution potential from nonpoint sources of pollution; integrating groundwater quality assessment models with spatial data to create spatial decision support systems; modeling groundwater movement: advection and dispersion modeling, developing flow field or vector fields representing groundwater seepage velocities, tracking particle movement, and particle retardation; modeling solute transport and leaching; and evaluating soil salinity and salt loading into groundwater (Delleur, 1999).

Several studies have applied GIS techniques to develop monitoring schemes (Bajarska et al., 2004), relate contamination to health risks (Harris, 1997; Kamilova et al., 2007), and assess vulnerability for contamination and exposure risk in groundwater (FDH, 2003; Dixon, 2005; Antonakos and Lambrakis, 2007), and surface water (Kelsey et al., 2004; Sauer et al., 2007). Harris (1997) used GIS technologies to analyze potential human exposure pathways caused by flooding of hazardous material sites in Georgia after the Alberto Flood of 1994. The analysis required the identification of flooded areas followed by step-by-step analysis integrating the source, transport media, exposure points, routes of exposure, and receptor population.

Hargrove and others (1996) generated a GIS-based risk evaluations by referencing specific environmental data collected at different locations. Risk analyses must deal with widely disparate types of data, including multiple contaminants sampled from multiple locations at different intervals (Hargrove et al., 1996). One approach used to convey multivariate data spatially was to create a series of hybrid maps which are combinations of charts and maps. Another approach taken was to collapse the multiple dimensions of contaminant data down to the single common currency of human health risk. The ultimate extrapolation of this collapsing approach resulted in a “Map Spreadsheet" in which arrays of maps of risk were spatially summed

across rows and columns (Hargrove et al., 1996). Hassan and others (2003) used GIS technologies to analyze the spatial risk pattern of arsenic in groundwater. They explored and mapped risk zones in order to understand the health effects and estimate the population risk over the area. Wycisk and others (2003) built a GIS-based 3D model, including geology, contaminants, hydrogeology, land-use and protected areas, for a risk-based approach in the implementation of remediation strategies of contaminated megasites.

Several studies have used GIS in vulnerability assessments (e.g. Babiker et al., 2005; Thapinta and Hudak, 2003; Nobre et al., 2007). One of these studies delineated areas that are more susceptible to contamination from anthropogenic sources, combining DRASTIC model and GIS. This technique provided efficient environment for analyses and high capabilities of handling large spatial data (Babiker et al., 2005). Thapinta and Hudak (2003) employed GIS technology to evaluate the vulnerability of groundwater to pesticide pollution using vulnerability factors. These factors were reclassified to a common scale, and a weighted average was computed to yield a vulnerability score. Groundwater vulnerability maps were generated for several pesticides. The groundwater vulnerability maps are effective for identifying locations warranting more detailed groundwater pollution and vulnerability investigations (Thapinta and Hudak, 2003). Nobre et al., 2007, used GIS in the assessment of groundwater vulnerability and risk mapping, based on a source–pathway–receptor approach. A modified version of the DRASTIC methodology was used to map the intrinsic and specific groundwater vulnerability. DRASTIC is a methodology which allows the pollution potential of an area to be systematically evaluated optimizing the use of existing data. It has two major portions: the designation of hydrogeologic settings and the superposition of a relative ranking system called DRASTIC. The hydrogeologic settings incorporate the major hydrogeologic factors (Depth to water, net Recharge, Aquifer media, Soil media, Topography, Impact of vadose zone and hydraulic Conductivity) which are used to infer the potential for contaminants to enter groundwater. The relative ranking scheme uses a combination of weights and ratings to produce a numerical value (DRASTIC index), which help to prioritize areas with respect to pollution potential (EPA, 1987b). A fuzzy hierarchy was adopted to evaluate the potential contaminant source index, including diffuse and point sources. A delineation of well capture zones was performed with

MODFLOW and MODPATH. The integration of these elements provided the mechanism to assess groundwater pollution risks and to identify areas that must be prioritized in terms of groundwater monitoring and restriction on use (Nobre et al., 2007).

Lucas and Jauzein (2008) evaluated spatial distribution patterns of concentration variations for chlorinated solvents in groundwater based on principal component analysis and GIS tools. They used a new exploratory statistical method called the Variability Index Method (VIM). The application of this method provided a useful assessment of controls over contaminant concentration variations as well as support for remediation techniques (Lucas and Jauzein, 2008). On another study, Dixon (2005) generated contamination potential maps by using detailed land use/pesticide and soil structure information in conjunction with selected parameters from the DRASTIC model. He incorporated GIS, GPS, remote sensing and the fuzzy rule-based model to generate groundwater sensitivity maps, and compared the results of our new methodologies with the modified DRASTIC Index (DI) and field water quality data (Dixon, 2005).

2.6 Groundwater Flow and Solute Simulation in the Upper North Coast Limestone Aquifer, Puerto Rico

Several groundwater flow simulations have been made in the karst aquifer system of Puerto Rico. Sepúlveda (1999) made a groundwater flow and solute transport simulation in the upper karst aquifer in Vega Alta, Puerto Rico. He made a three-dimensional groundwater flow and solute-transport model to evaluate the effects of remedial alternatives designed to reduce the magnitude and extent of trichloroethylene (TCE) plume in the water table aquifer. Heads measured from February 1983 to April 1992 were used to calibrate the groundwater flow component of the model. TCE concentrations measured in groundwater samples in January 1990 and March 1992 were used to calibrate the solute-transport component of the model. Remedial alternatives were simulated to study the movement of the TCE plume from March 1992 to March 2022. TCE mass in the Vega Alta water table aquifer was estimated to be 12,814 pounds in March 1992 and the remaining in the aquifer in March 2022 after simulating the alternatives ranges from 5,720, to 3,689 depending on the remedial alternative. Measured TCE concentrations suggest an overall movement of the plume toward the northeast at altitudes above

-125ft. TCE concentrations between altitudes of -225 and -285ft indicate the plume has spread both east and west (Sepúlveda, 1999).

In a simulation of the water table aquifer in Manatí-Vega Baja aquifer, Cherry (2001) made a steady state two-dimensional groundwater flow model to improve the understanding of the unconfined upper aquifer within the north coast of Puerto Rico, between Manatí and Vega Baja. The study assumed a regional-scale diffuse groundwater flow. The study showed that the increased in groundwater withdrawals from 1.0 cfs for 1940 to 26.3 cfs in 1995, had reduced the natural groundwater discharge to springs and wetland areas, and induced additional recharge from the rivers (Cherry, 2001).

In another study, Torres-González (1996) made a quasi-three-dimensional finite-difference, groundwater flow model. The study showed that most ground-water recharge to the upper aquifer occurs in the outcrop area of the Aguada Limestone and generally flows north through the Aguada Limestone into the Aymamón Limestone. The study assumed a regional-scale analysis in which diffuse flow dominates and conduit flow is assumed negligible (Torres-González, 1996).

3 Objective

The overall objective of this project is to assess potential contaminant exposure paths in the karst groundwater system of northern Puerto Rico using geographic information systems (GIS) technologies. It further aims to develop improved methods for predicting human exposure through karst aquifer using GIS technologies. The project focuses in potential path for exposure of chlorinated organic chemicals in Vega Alta-Dorado area, part of La Plata-Arecibo hydrological system.

4 Methodology

The primary goal of this project is to assess potential contaminant exposure paths in the karst groundwater system of northern Puerto Rico using GIS technologies, with the reconstruction of potential path contaminated with chlorinated solvents. These contaminants were released from contaminated sites in the karst groundwater system in the La Plata-Arecibo region in northern Puerto Rico (Figure 2-2). This goal was attained through integration of spatial hydrogeologic, hydrologic, and contaminant concentration data using GIS technologies. Data was collected from several sources, evaluated, and incorporated in the ArcMap database. It was assumed to be constant over time. Data characteristics were overlain and analyzed within the context of a number of basemap using ArcGIS 8.3 (ESRI, 2003). This GIS platform uses intelligent data models for representing geographical features, and provides the necessary tools to create and work with spatially-distributed data (ESRI, 2001). The spatial analyst extension for ArcGIS was used to perform the analysis. The analysis involved the development of groundwater velocity vectors, which influence the direction and magnitude of contaminant transport. The groundwater system was assumed to be represented by equivalent porous media and solute transport to be 2D. Dispersivity theory assuming Gaussian distribution was utilized to estimate the lateral extent of potential contamination along the velocity vectors. Vectorial and lateral extent of contamination was thereafter overlain on maps containing the spatial distribution of wells where target contaminants have been detected. Because the purpose of the study is to determine the potential pathway, instead of modeling the contaminant transport, the only mechanisms considered were advection and dispersion.

4.1 Data Collection

Physical features, as well as hydrogeologic, hydrologic, and contaminant concentration data was collected for the upper unconfined aquifer in the north coast of Puerto Rico. The study focused on phthalates and chlorinated volatile organic compounds (VOCs) including TCE, PCE, Chloroform, 1,1,2-Thrichloroethane, Carbontetrachloride, Methylene Chloride, 1,1-Dichloroethane, 1,1,1-Trichloroethane, 1,2-Dichloroethane, 1,1-Dichloroethylene, 1,2-trans-dichloroethylene, DEP, DBP, DEHP, Benzyl-n-butyl phtalate, Dimethyl phthalate, Di-n-octyl

phthalate. Phthalates are a significant emerging contaminant found in Puerto Rico, and chlorinated VOCs are ubiquitous, also, in Puerto Rico. Data was collected for the Arecibo to Toa Baja area (Figure 2-2).

Base map data included: municipality boundaries, geology, groundwater potentiometric level, surface hydrology (rivers, wetland, and coast), hydraulic conductivity and porosity maps and aerial photos. Point data included well and spring location, water levels, and contamination data, superfund sites (active and deleted) (EPA, 2010a; EPA 2010b), landfill location, and the EPA toxic release inventory (EPA, 2010c).

Base map information on Puerto Rico's shape and municipality boundaries (Figure 4-1a), hydrology (Figure 4-1b) and geology (Figure 4-1c), were obtained from the Puerto Rico Water and Environmental Institute (PRWEI, 2007). The hydrology and geology maps for the north-coast study area are shown in figure Figure 4-2b and Figure 4-2c, respectively.

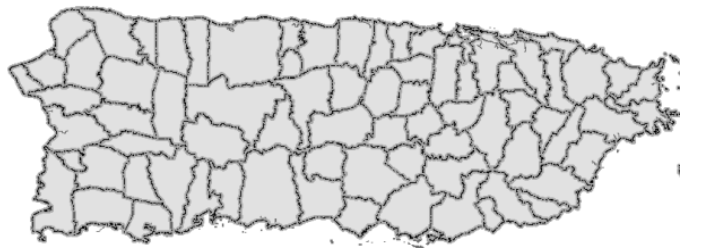

(a)

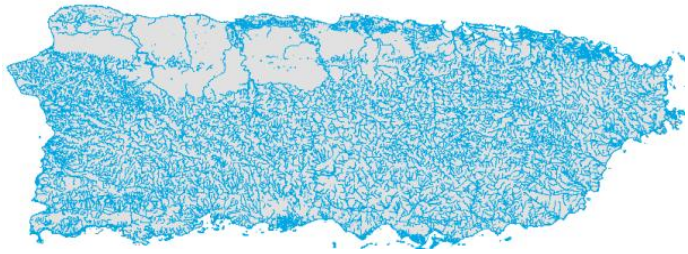

(b)

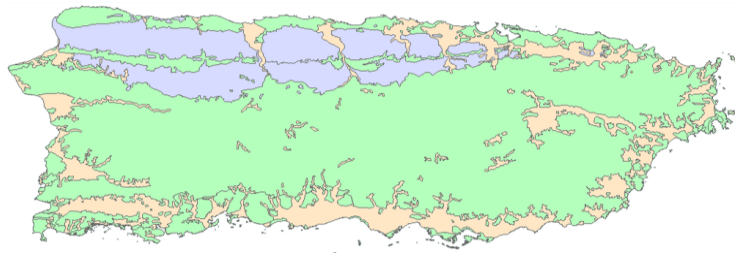

(c)

Figure 4-1: (a) Puerto Rico's shape and municipality boundaries; (b) hydrology; (c) geology (source: PRWEI 2007)

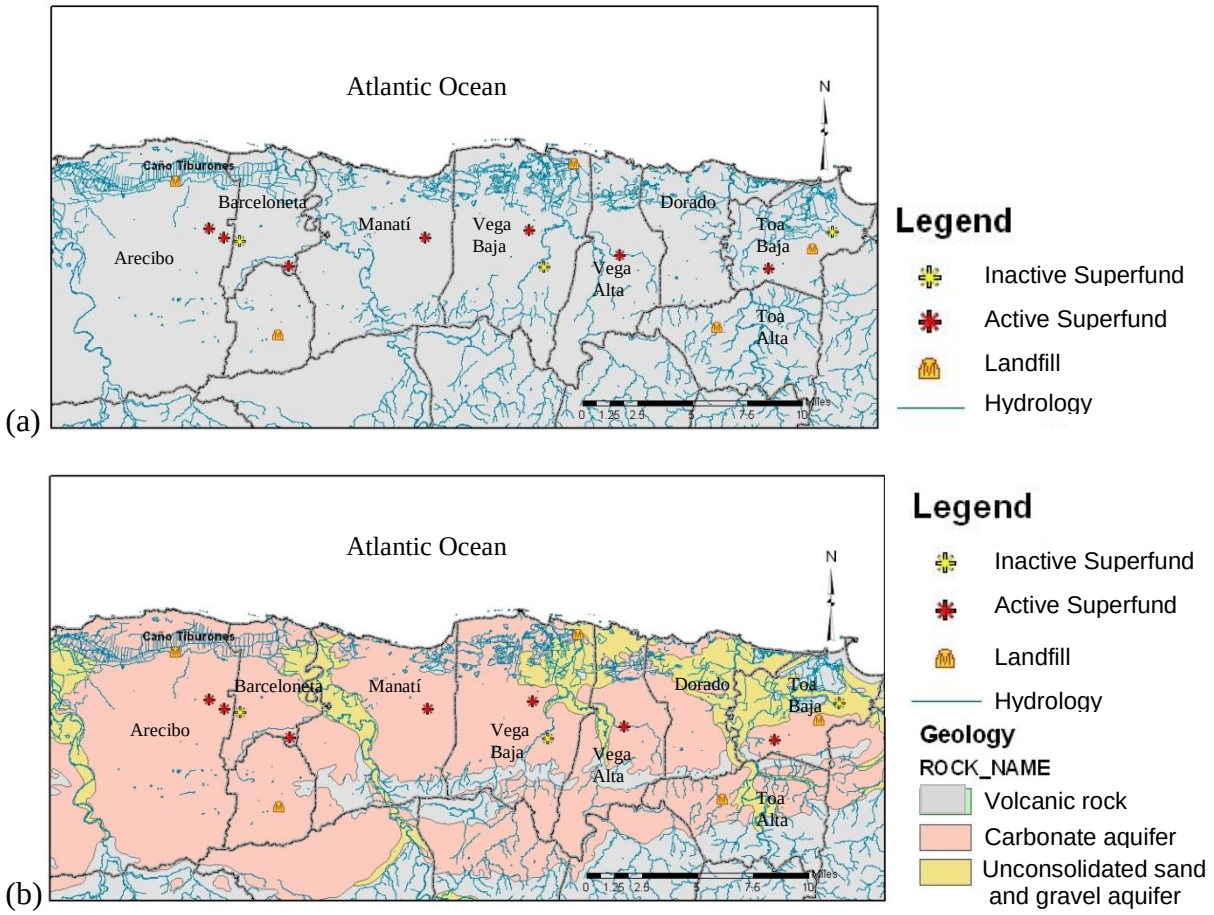

Figure 4-2: (a) North-coast study area hydrology map and (b) geologic map.

Potentiometric water levels (Figure 4-3) and hydraulic conductivities (Figure 4-4) were obtained from Renken et al. (2002) and Sepúlveda (1999). Contamination data was obtained from USGS internet data base (USGS, 2008), USGS water resource investigation reports (Guzman-Rios and Quinones, 1984; Guzmán-Rios and Quiñones-Márquez, 1985; Guzman-Rios et al., 1986; Sepúlveda, 1999) and EPA database (EPA, 2008a). The data include wells with detected chlorinated VOCs (Appendix B) and phthalates, their location and the detected concentrations. Information on wells with detection of metals and pesticides were also collected, but not included in this study. National Priority List site and Toxic Release Inventory site locations (Figure 4-5) were obtained from the Environmental Protection Agency website (EPA, 2010a; EPA 2010b; EPA 2010c).

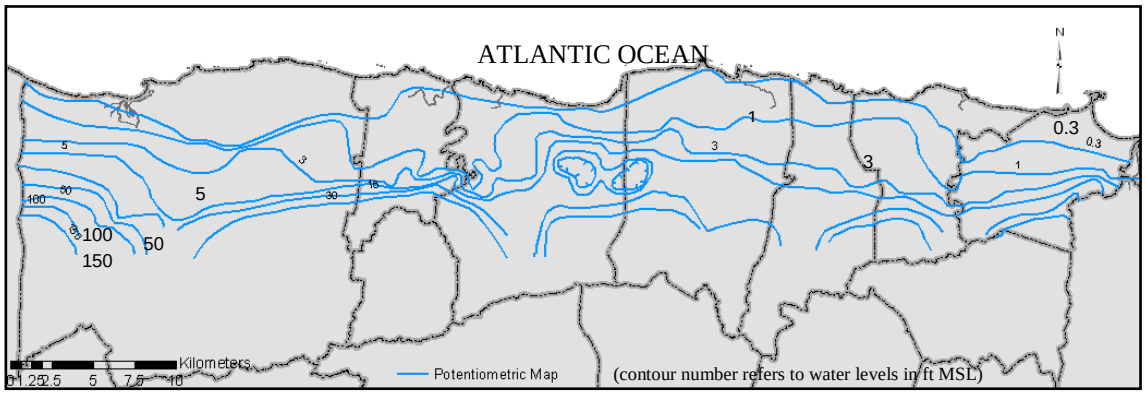

Figure 4-3: Arecibo to Toa Alta potentiometric map of upper aquifer in Arecibo to Toa Baja area (Source: Renken et al. 2002)

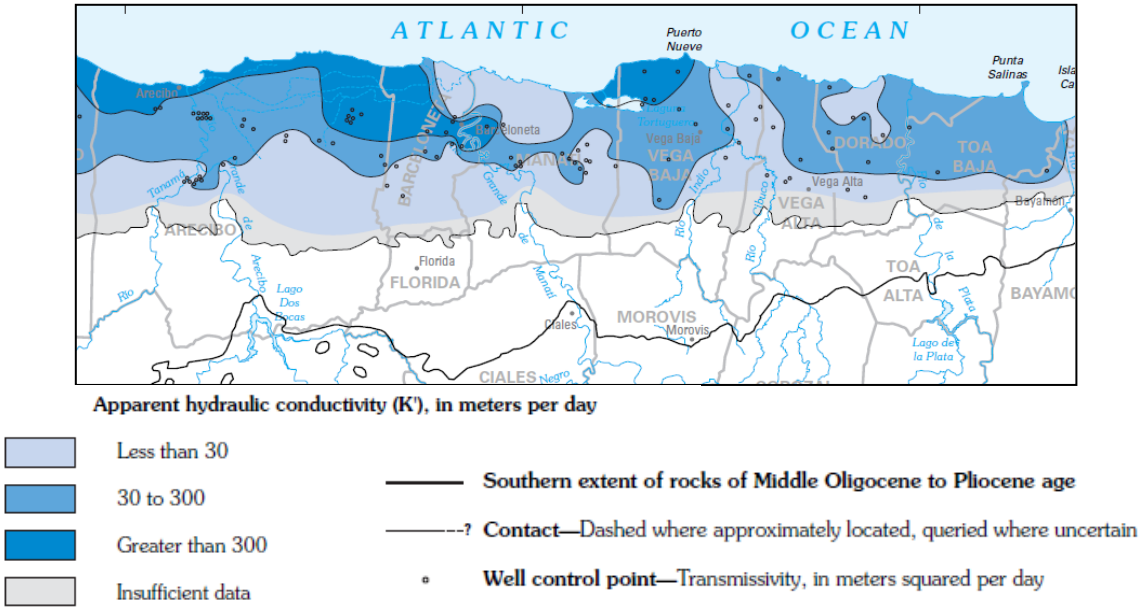

Figure 4-4: Renken's distribution of hydraulic conductivity in the north-coast study area. (Source: Renken et al. 2002)

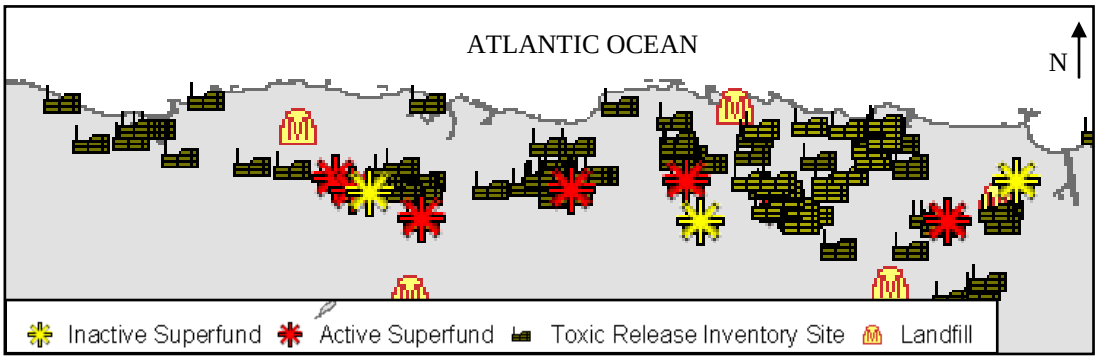

Figure 4-5: National priority list sites, toxic release inventory sites and landfills in Arecibo to Toa Baja area (Source: EPA 2010)

Other pertinent data, such as wetland and aquifers distribution and census data were downloaded from GIS Depot (USGS, 2010) and/or provided by the GIS office of the Puerto Rico Planning Board (PRPB, 2008). The location of water intakes and distribution lines (Figure 4-6) where provided by the Puerto Rico Aqueduct and Sewer Authority, PRASA (PRASA, 2008). Well and spring location and water levels were obtained from the National Water Information System: Web Interface (USGS, 2008), and from several published reports (Guzman-Rios and Quinones, 1984; Guzmán-Rios and Quiñones-Márquez, 1985; Guzman-Rios et al., 1986; Sepúlveda, 1999).

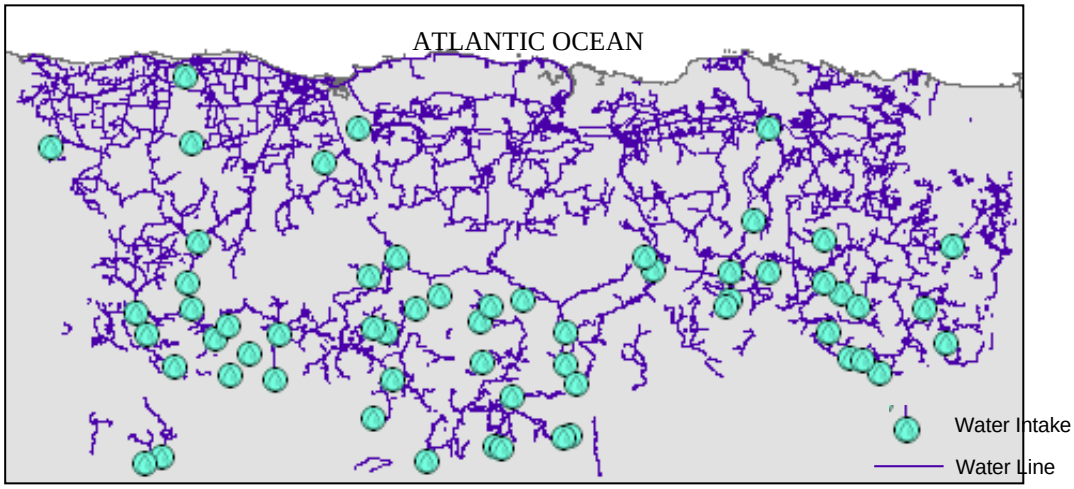

Figure 4-6: Water distribution system in Arecibo to Toa Baja area (Source: PRASA 2008)

Although most of the data was already revised and validated by the agencies and institutions, all the collected data was revised again for accurateness and system representativeness. Once revised, the data was incorporated in the ArcMap database.

4.2 Methods

Construction of potential contamination paths in the upper aquifer of the North Coast was based on evaluation and integration of collected hydrogeologic, hydrologic, and contaminant concentration data, using GIS technologies. Once collected and revised, the data was incorporated into the ArcMap database. Data was segregated into characteristic path parameters, including contaminant presence and concentrations, water levels, porosity and hydraulic gradients. Values were assumed constant over time. Spatially-distributed data characteristics

were used to develop velocity vectors, time of travel, and lateral extent of contamination from particular contamination sources. Because the purpose of the study is to determine the potential pathway, instead of modeling the contaminant transport, the only mechanisms considered were advection and dispersion.

The assessment assumed steady-state conditions in an isotropic and vertically homogeneous aquifer. At the scale of the analysis (1in=100,000in) and steady-state condition, it was assumed that the karstic aquifer can be described as equivalent porous media. This has been in fact the assumption made by several numerical groundwater flow models developed for the north coast of Puerto Rico (Torres-González, 1996 and Cherry, 2001).

The proposed methodology was applied to the Vega Alta-Dorado area within the Arecibo – Toa Baja hydrogeological system (Figure 4-7). This area was selected because it has a greater density of contamination and hydrogeologic data in the study area.

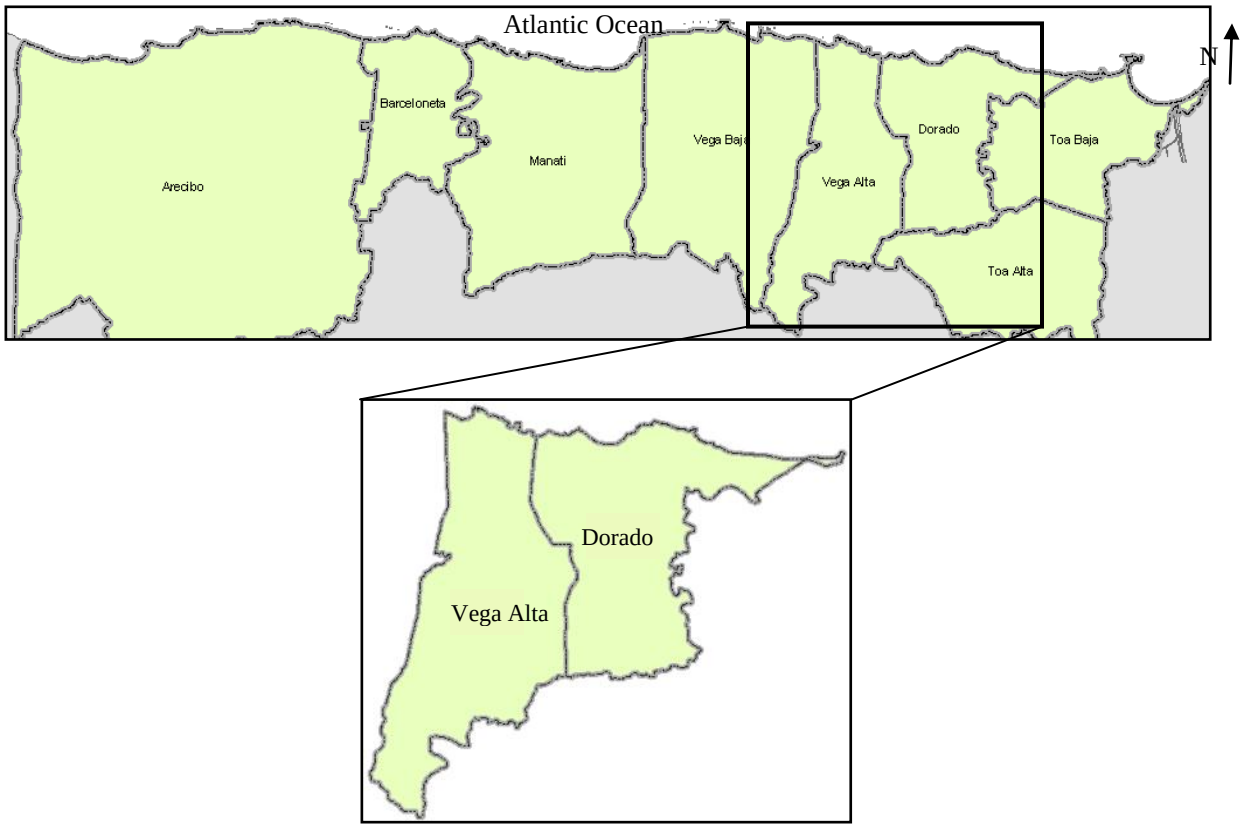

Figure 4-7: Vega Alta-Dorado study area.

4.2.1 Velocity Vector Distribution

Darcy's velocity distribution in the Vega Alta – Dorado area was estimated from equation (1) as the product of the hydraulic gradient and hydraulic conductivity base maps (Figure 4-8a). The advection velocity distribution was estimated from equation (2) as the gradient of Darcy's velocity map and porosity base maps (Figure 4-8b). Base maps were prepared by digitizing and georeferencing the hydraulic head (Figure 4-8a), hydraulic conductivity (Figure 4-8b) and porosity maps Figure 4-8c), developed by Sepúlveda (1999). The *Editor Tool* in ArcGIS was used for this purpose. These maps were digitized in ArcGIS and then converted to raster with the *Convert Features to Raster* option in Spatial Analyst. Head values in between contour levels were determine using a spline interpolation method provided by ArcGIS Spatial Analyst. Spline interpolation was applied because it yields smoother results (ESRI, 2001). To perform the interpolation, water level data were added as a layer into the program as tabular data, and converted to shapefile. Interpolation was performed using an analysis mask and extent from 66°21'32"W to 66°15'19"W and 18°29'04"N 18°24'50"N. These settings are adjusted in the *Options* menu of the Spatial Analyst extension. Hydraulic gradients were estimated as the difference in hydraulic heads over the length of the cell (30m), which integrates the spatial resolution at which the Darcy's velocity is being estimated. Hydraulic conductivity and porosity distribution were digitized as block distributions obtained from Sepúlveda (1999) (Figure 4-8b and Figure 4-8c).

Groundwater flow direction was determined from the head raster layer. The elevation at any point on the water table equals the energy head. Flow occurs from areas of high energy to low energy. For isotropic media, flow lines lie perpendicular to head contours (Todd and Mays, 2005). The flow direction was determined by creating a vector map from the head layer in Surfer® (Golden Software, 2008). To create the vector map, the head layer was exported from ArcGIS® to Surfer®. The vector map was created using the 1-Grid Vector Map tool. When using this tool a grid file must be selected in the Open Grid dialog, then the map is created. Because the raster files converted by ArcGIS were in ESRI Grid format, which were not supported by Surfer, it was necessary to convert ESRI Grid to XYZ data. A Microsoft Visual Basic code tool downloaded from ESRI (Fried, 2003), was used to convert raster to XYZ data.

This kind of data can be read by Surfer, which then converts to Surfer Grid (.grd). The direction of the water table heads were plotted using the *1-GRID vector map* button tool in Surfer®. Peculiarities on the use of this code are described in Appendix A. The vector map developed with Surfer® was exported to ArcGIS, and used to represents the direction of groundwater flow.

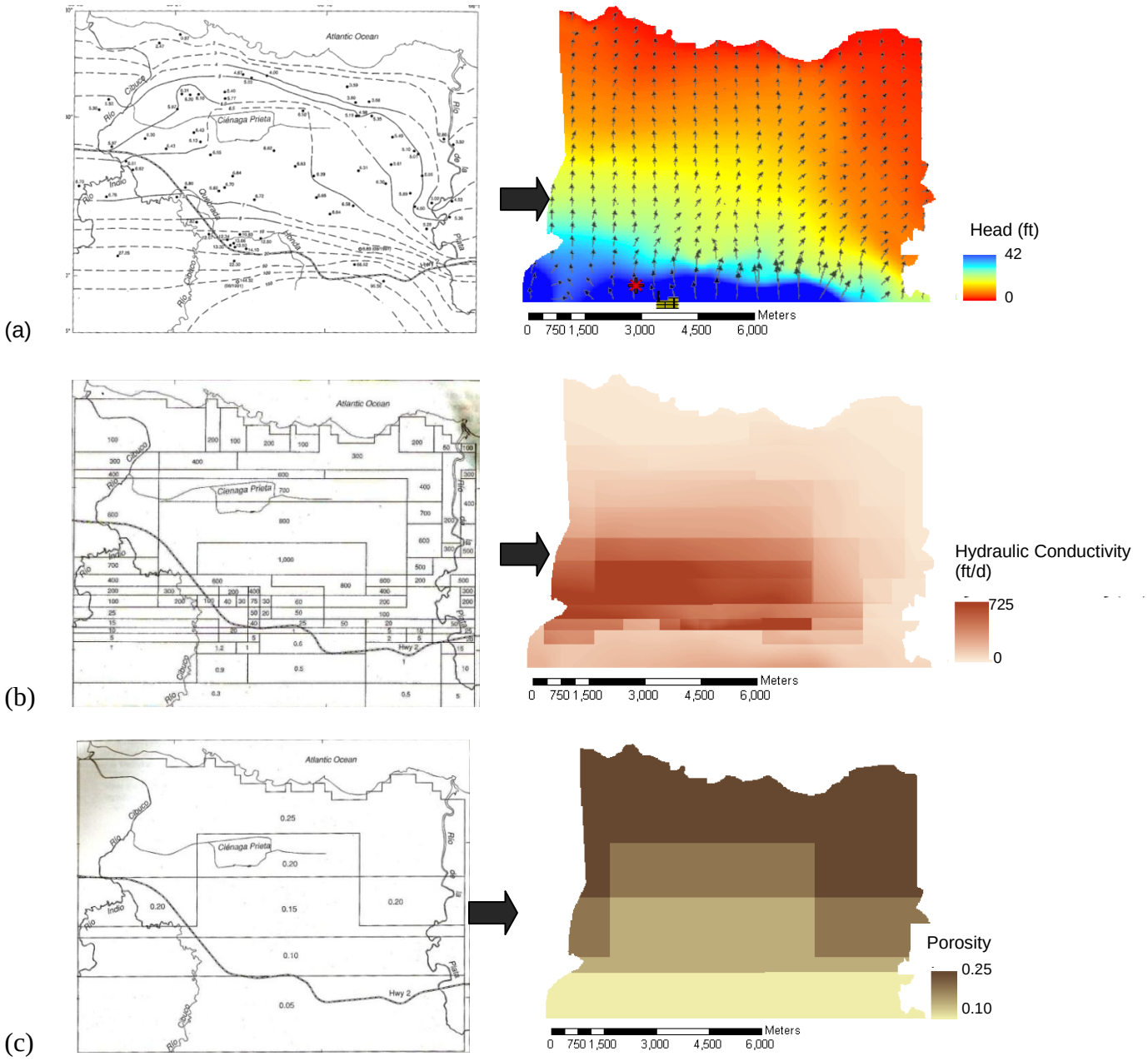

Figure 4-8: (a) Water level contour map from Sepúlveda, 1999 converted in head map with velocity direction vectors, (b) Hydraulic conductivity map from Sepúlveda, 1999 converted in a digital equivalent hydraulic conductivity map and (b) porosity map from Sepúlveda, 1999 converted in a raster porosity map.

The longitudinal direction of path was established from a given source of contamination along the direction of groundwater flow vectors developed from the raster calculations. The longitudinal path was drawn using a polyline with the *editor tool*. The line followed the velocity vector estimated from the groundwater direction layer and the potentiometric map. The source of contamination was set as the starting point of the spread, which in this case was the Vega Alta Public Supply Well superfund site. The longitudinal extent of contamination was extended to near the coast because enough time has passed since the proposed listing (1983) of this superfund site, therefore the contaminant could have reached the coast. Sorption process could have played an important role at early times after the release because it could have slowed down the movement of the contaminant. It is assumed that enough time has passes for contaminant breakthrough. Transformation processes, such as biodegradation, hydrolysis and oxidation-reduction reactions, influence mainly the concentration of the contaminant, and not its path. For this reason those processes are not considered in this study.

4.2.2 Lateral Extent of Contamination

The lateral extent of contamination was estimated along the longitudinal direction of the path by calculating the transverse standard deviation of the plume (equation 3) at several points along the path, corresponding to the time of travel from the contamination source. The standard deviation represents the lateral extent of the spreading. The transverse dispersion (D_T) coefficient was calculated used equation 5 with negligible molecular diffusion. The transverse dispersivity was initially assumed to be 16 ft (5 m) (Dassargues and Derouane, 1998). In the literature, there were transversal dispersivity values for karstified limestone aquifers from as low as 0.5 ft (Sepúlveda, 1999) to as high as 52 ft (Batu, 2006). Between these values, another source (Dassargues and Derouane, 1998) had an intermediate value of 16 ft. This is precisely why this value was selected as the initial transversal dispersivity, because it was an intermediate value. In the analysis, the dispersivity value was varied to determine the effect of this value on the potential path of contamination. D_T was estimated for each point along the advective path by using the velocity vector at each point and a cumulative time of travel (**t**) was assumed to be the time it takes a particle to travel from one point to another. This was done by dividing the length

between any two points by the average linear velocity and adding it to previous time travel. All calculations were performed in Excel spreadsheets.

The lateral extent of contamination along the longitudinal direction was assumed to be represented by a width equal to 4σ, which represents 95.44% of the area under the Gaussian curve (Ott and Longnecker, 2001). The extent was estimated as the 4σ from the longitudinal direction at calculated average travel times. Once, the longitudinal direction and spreading extension were calculated and converted in layers, the potential pathway map was created in ArcGIS®. At each point where the lateral extent was calculated, a buffer zone with that value was created with the Buffer Wizard. Those buffer zones were used to delineate the potential contamination pathway.

4.3 Potential Path of contamination in the Vega Alta – Dorado Area

The proposed methodology was applied to the Vega Alta – Dorado area within the Arecibo and Toa Baja hydrogeological system (Figure 4-7). Groundwater velocity vectors for the Vega Alta – Dorado area were calculated as the product of hydraulic gradients and equivalent hydraulic conductivity, divided by the porosity (equation 2) raster files. Hydraulic gradients were estimated using the potentiometric water elevation, developed by Sepúlveda (1999). The hydraulic conductivity and porosity distribution were also estimated using the data reported by Sepúlveda (1999). In Sepulveda's report, the aquifer was divided in several layers, and information of K was provided for all layers. Each hydraulic conductivity layer was digitized in ArcGIS in order to calculate the equivalent hydraulic conductivity. Since, flow direction was parallel to the layers and it was assumed that each layer was individually isotropic and homogeneous; the equivalent horizontal hydraulic conductivity was calculated using the following equations:

$$K_{eq} = \frac{K_1 z_1 + K_2 z_2 + \ldots + K_n z_n}{z_1 + z_2 + \ldots + z_n} \quad \textbf{(7)}$$

where,

K_i = Hydraulic conductivity of each layer

z_i = Thickness of each layer

n = Number of layers.

The thickness of all layer were the same (Sepúlveda, 1999), so the equation could be simplified to:

$$K_{eq} = \frac{K_1 + K_2 + ... + K_n}{n} \quad \textbf{(8)}$$

After digitizing all layers, they were converted to raster (Figure 4-8b) in order to be able to use it in the raster calculator.

The longitudinal direction of the path was established from a given source of contamination along the direction of groundwater flow vectors developed from the raster calculations. The source of contamination for this project was set at the Vega Alta Public Supply Well superfund site (See Figure 4-9). The starting point was simulated in two locations: at the superfund ID location (EPA 2010b), and at location of the Caribbean General electric (CGE) (Figure 4-9), which has been identified as the contamination Responsible Party (EPA, 1999).

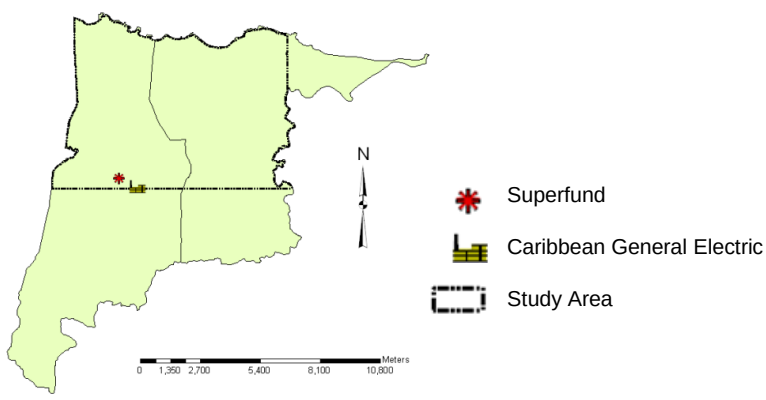

Figure 4-9: Vega Alta Public Supply Well superfund site and Caribbean General Electric site in study area.

The lateral extent of contamination was estimated from the standard deviation (equation 3) of the concentration distribution along the spatially-variable mean. Transverse dispersion was estimated as a function of dispersivity (equation 5). Initially, the dispersivity was assumed to be 16 ft (5 m). This value was subsequently varied to capture maximum and minimum values reported for karstified limestone aquifers (Sepúlveda, 1999; Batu, 2006). The analysis was made for a maximum dispersivity value of 52 ft (16 m) in transversal direction and 170 ft (52 m) in

longitudinal direction (Batu, 2006). Also, a minimum value of 0.5 ft (0.15 m) in transversal direction and 10 ft (3 m) in longitudinal direction (Sepúlveda, 1999) was analyzed in order to observe how the pathway extent would change when varying dispersivity values. Another pathway was delineated using the scale-dependent dispersivity relationship, $\sigma_L = 0.1L$ (Gelhar et al., 1979), along the longitudinal path from the point source (L).

5 Results

Results from Vega Alta-Dorado area are presented in a set of figures that were developed using ArcGIS. These figures present the results obtained with the methodology proposed to delineate the potential pathway of the contaminants, released by the contamination source in the study area.

5.1 Vega Alta – Dorado Area

Groundwater velocity vectors were generated from head, hydraulic conductivity, and porosity layers. The head distribution and vector layer generated for the Vega Alta – Dorado area is shown Figure 5-1. It shows that groundwater tends to move toward the north, with some components moving toward the Río La Plata on the eastern side of the study area.

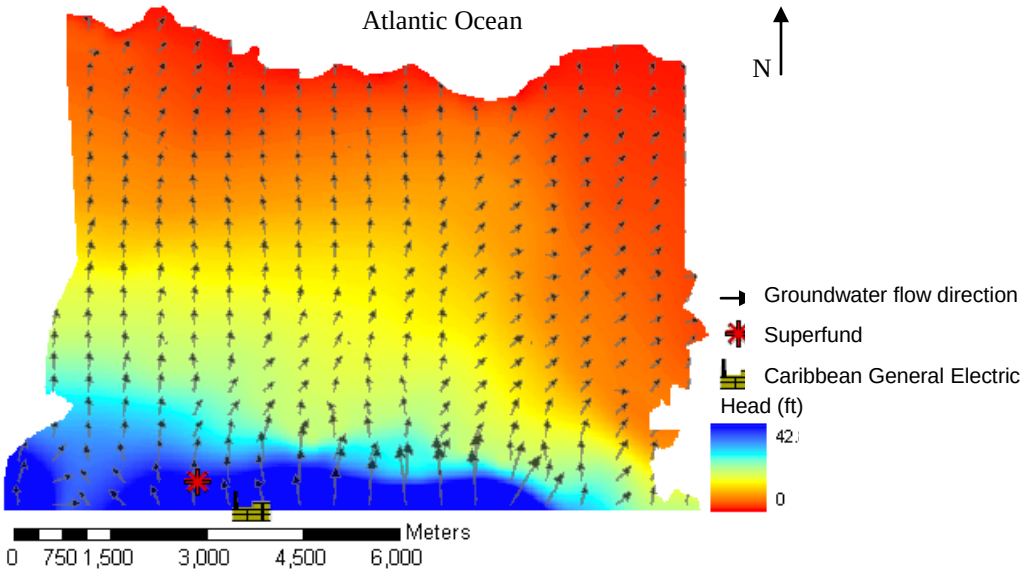

Figure 5-1: Head distribution and vector layers

The equivalent hydraulic conductivity layer is shown in Figure 5-2. It shows spatially-variable values ranging between 10 and 725 ft/d.

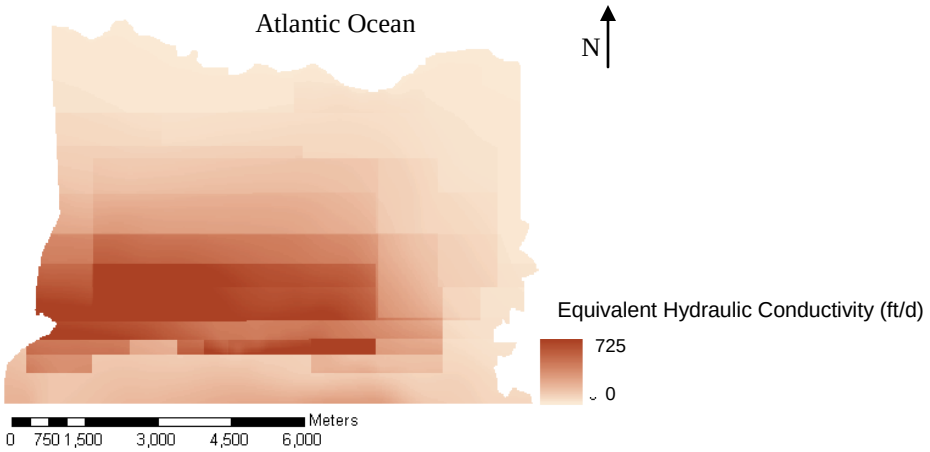

Figure 5-2: Vega Alta - Dorado equivalent hydraulic conductivity map

The product of the head gradient and equivalent hydraulic conductivity (K) distribution yields the Darcy's velocity distribution (Figure 5-3). Darcy velocity values ranged from 0 ft/d to 90 ft/d, with a mean of 49.40 ft/d.

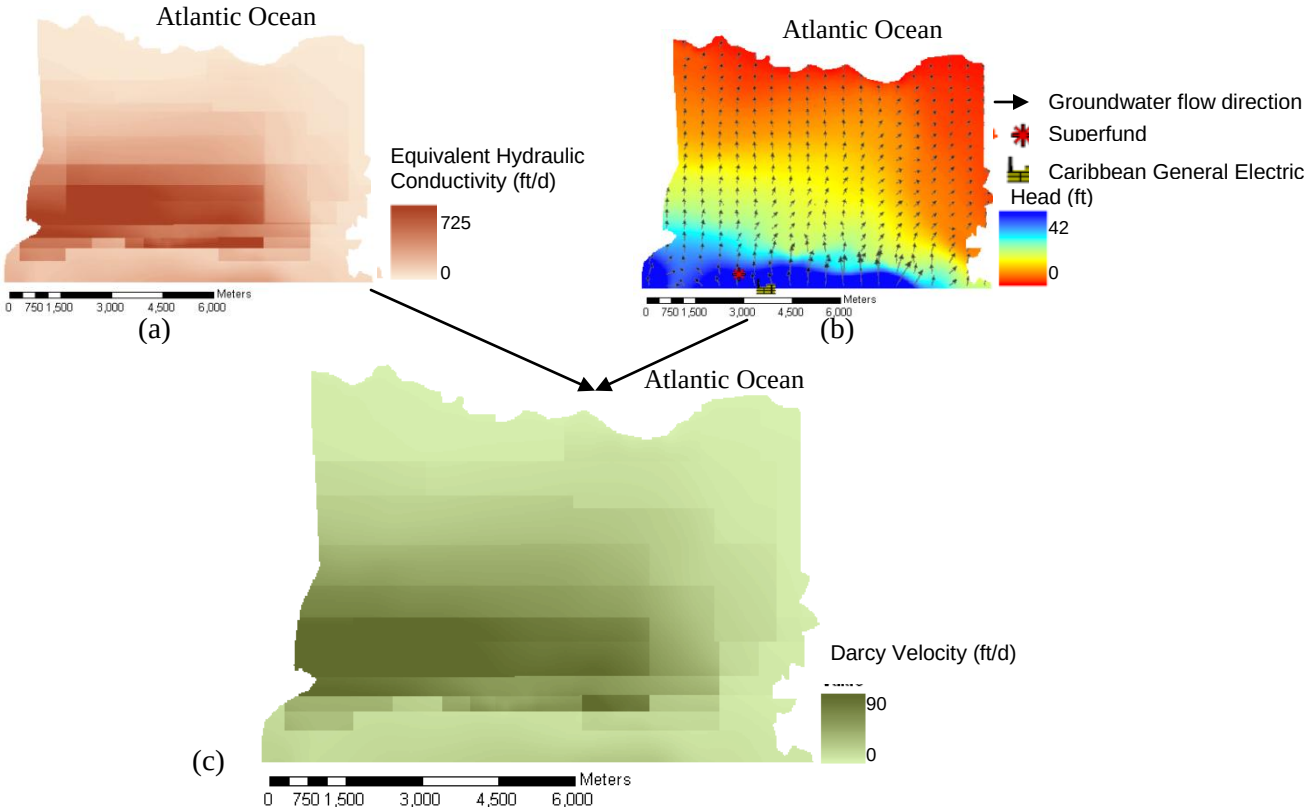

Figure 5-3: Equivalent Hydraulic Conductivity (a) and heads layers (b) used in the calculation of Darcy velocity (c)

The gradient of Darcy's velocity and the porosity layer (Figure 5-4) yields the average groundwater linear velocity distribution. The porosity distribution ranges in the study area between 0.10 and 0.25.

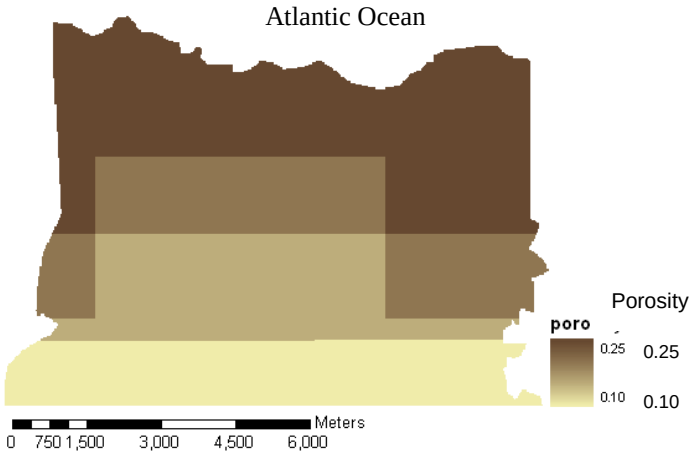

Figure 5-4: Raster porosity distribution applied in study area

The estimated groundwater velocity distribution is shown in Figure 5-5. This velocity ranges from 0 ft/d to 726 ft/d, with a mean of 230.63 ft/d.

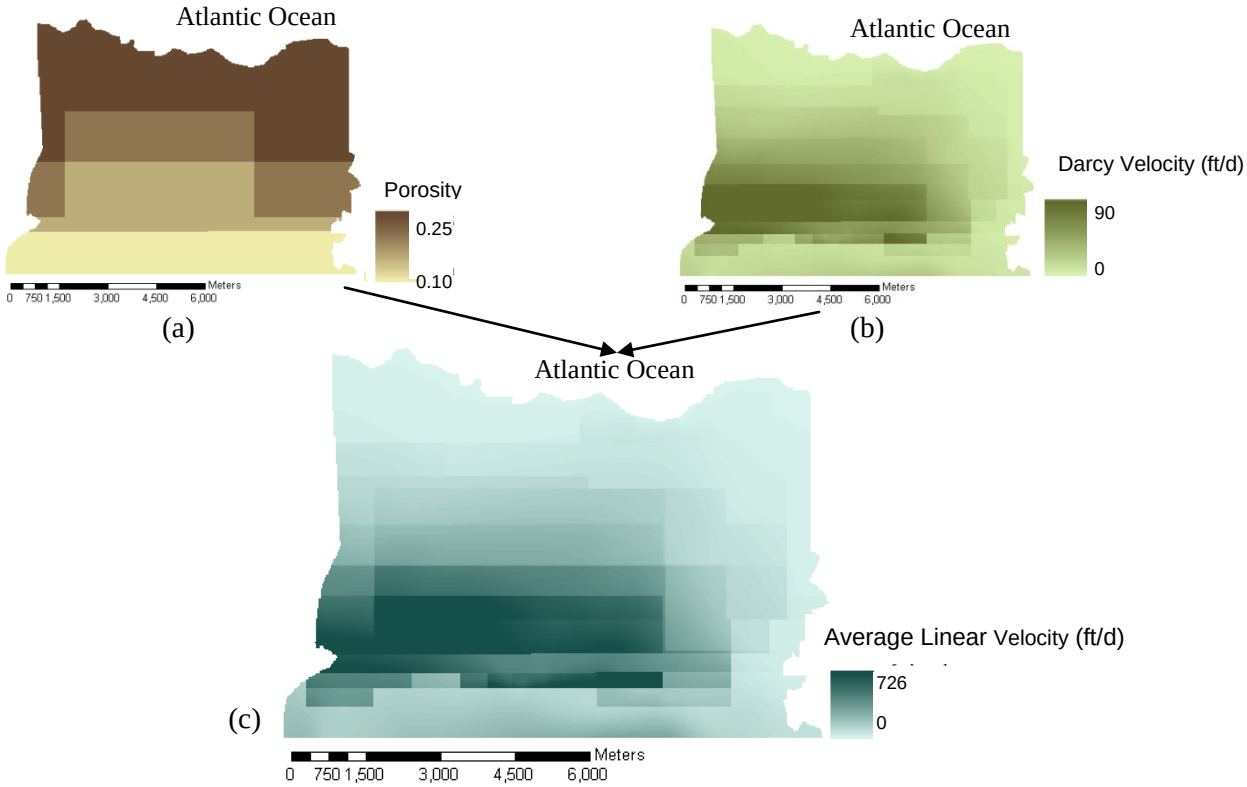

Figure 5-5: Porosity (a) and Darcy's velocity layers (b) yield average linear velocity map (c)

With the groundwater flow direction map and the heads contours maps, the advective flow direction was delineated in ArcGIS, as shown in Figure 5-6. This figure illustrates the longitudinal direction of the contaminant from the superfund site. It follows the groundwater flow direction going perpendicular to the head contours.

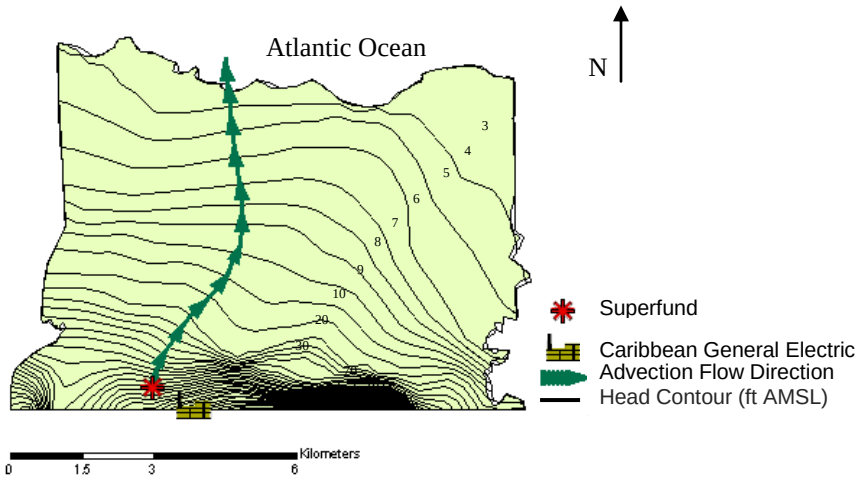

Figure 5-6: Longitudinal direction path

The extent of contamination from the superfund site is shown in Figure 5-7. In this analysis, the path is assumed to be only controlled by average advective and dispersive processes, and do not take contaminant properties, nor concentrations. Figure 5-8 shows the extent of contamination from the CGE facility and Figure 5-9 show the extent formed by both sources for the same dispersivity value (α_T=16 ft). In the following figures the pathway starting point will be at CGE facility, because it is the contamination responsible party and the contamination is supposed to comes from that point.

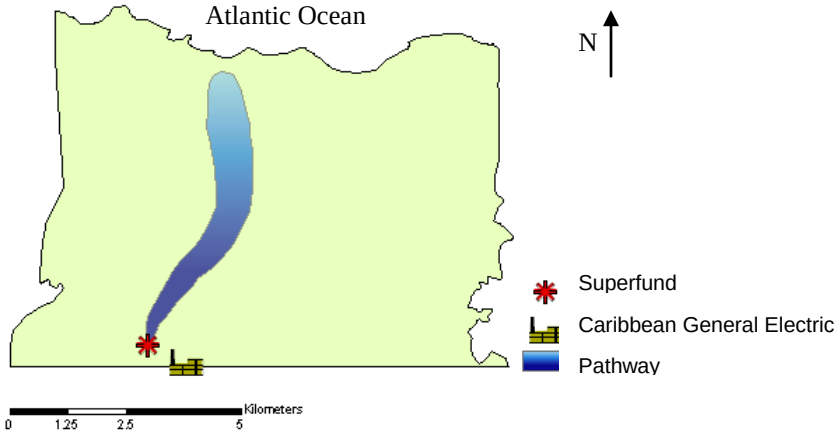

Figure 5-7: Spreading extent (α_T=16 ft) of contamination pathway from superfund site ID location

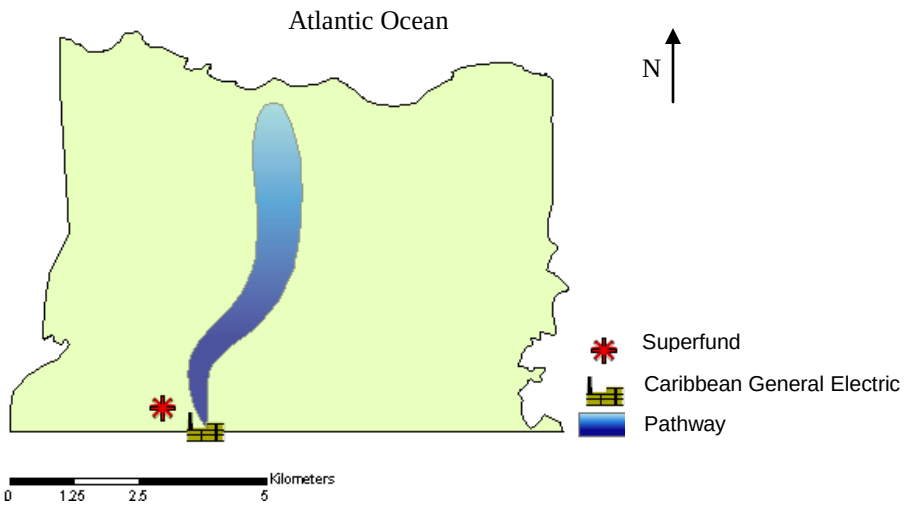

Figure 5-8: Contamination pathway (α_T=16 ft) from CGE

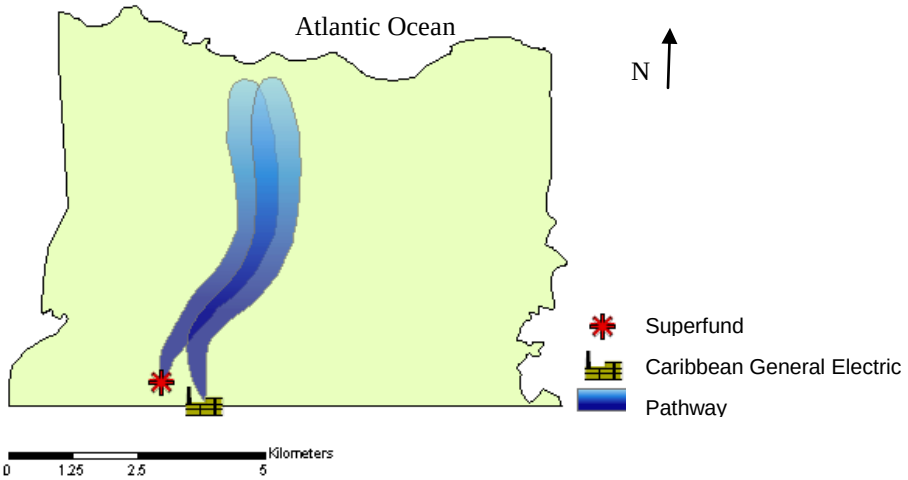

Figure 5-9: Contamination pathways from Vega Alta Superfund and CGE

The lateral extent of contamination from the longitudinal path depends on the dispersivity value used. Table 5-1 shows the standard deviation obtained by applying different dispersivity values to the velocity vector within the longitudinal path. The extent was assumed to be 4σ. Figure 5-10 and Figure 5-11 are the pathways delineated using the maximum and minimum dispersivity, from the sensitivity analysis.

Table 5-1: Standard deviation results with different dispersivity values

Dispersivity	*Average σ*	*Min σ*	*Max σ*	*Min Σσ*	*Max Σσ*
α = 16 ft	140 ft	58 ft	264 ft	145 ft	819 ft
α = min = 0.5 ft	25 ft	10 ft	47 ft	26 ft	145 ft
α = max = 52 ft	253 ft	104 ft	476 ft	261 ft	1476 ft
α = 0.1L	332 ft	81 ft	954 ft	93 ft	2145 ft

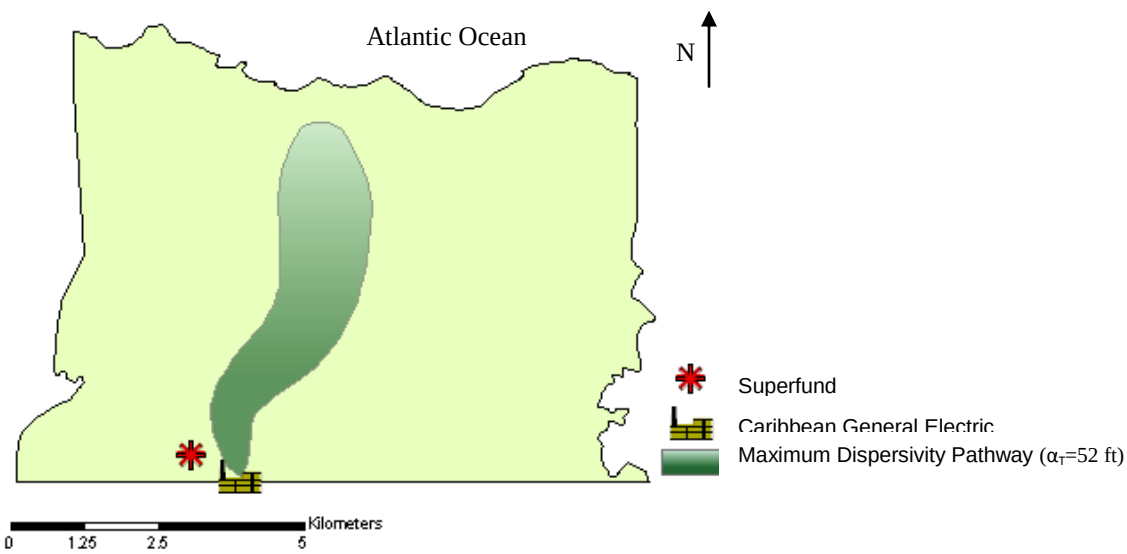

Figure 5-10: Contamination pathway from CGE with maximum dispersivity (α_T=52 ft)

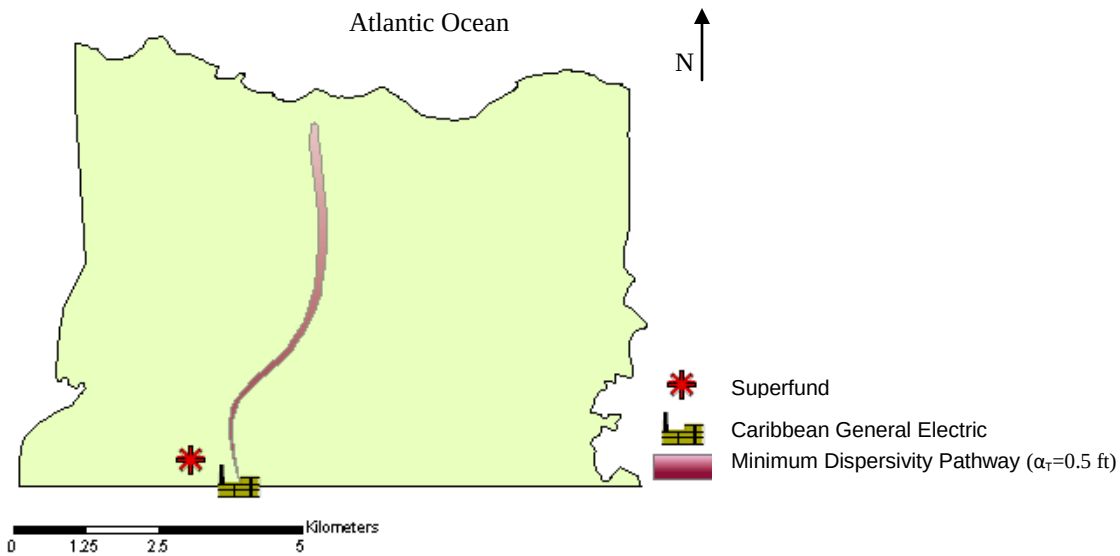

Figure 5-11: Contamination pathway from CGE with minimum dispersivity (α_T=0.5 ft)

Figure 5-12 shows the potential contamination pathways for maximum and minimum dispersivity values. The green pathway shows the pathway with the larger dispersivity value and the pink pathway with the smaller dispersivity value, both found in the literature.

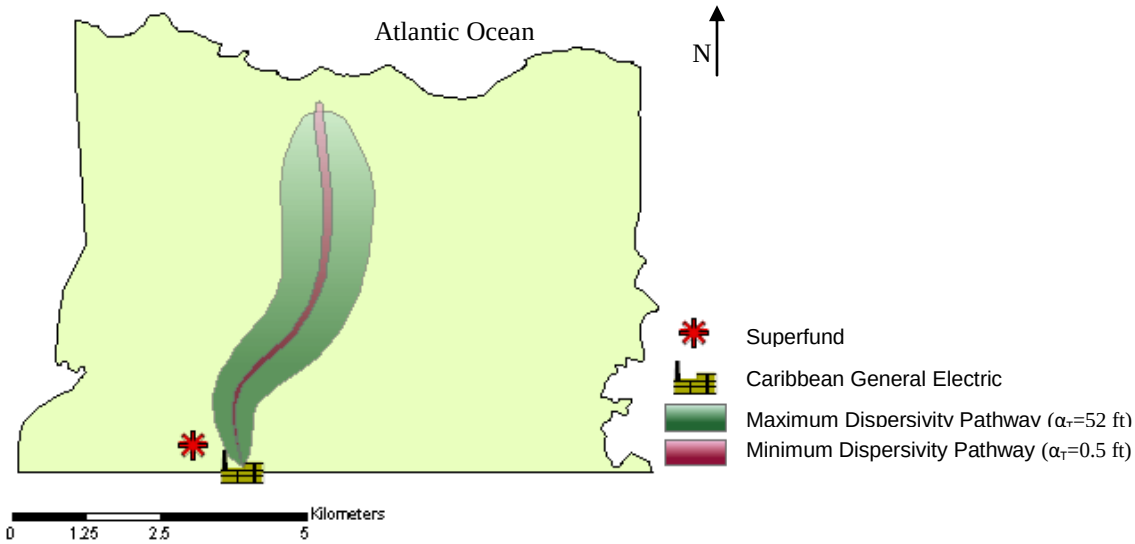

Figure 5-12: Contamination pathways with maximum and minimum dispersivity

Figure 5-13 shows the contamination pathway resulting from the delineation using the scale-dependent function (equation 7) to obtain longitudinal dispersivity. Transversal dispersivity was assumed 1/10 of the longitudinal value.

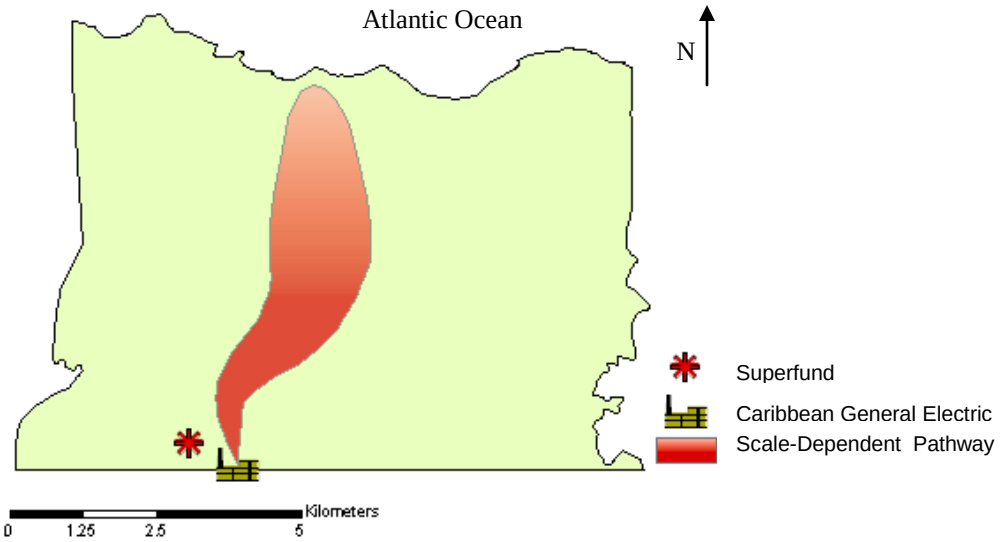

Figure 5-13: Contamination pathway from CGE with scale-dependent dispersivity

Figure 5-14 shows the extent of combination for different values of dispersivity used in the model. As expected, higher values yield greater extent of contamination. Scale-dependent and maximum values show similar behavior.

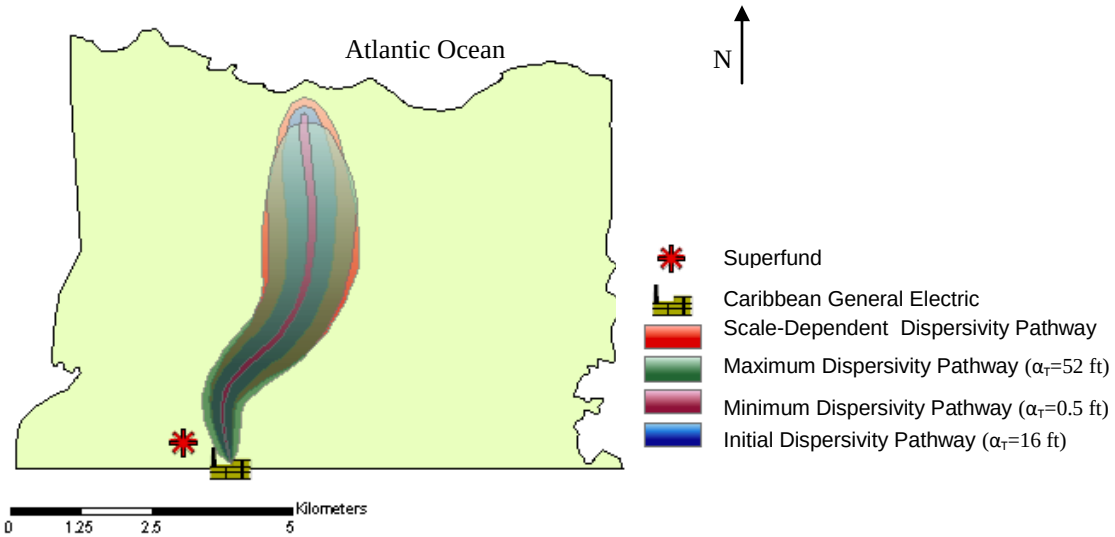

Figure 5-14: Combination pathway from CGE for variable dispersivity values

6 Discussion

In the Vega Alta – Dorado area, groundwater enters the system through surface infiltration and direct injection of runoff into karstic conduits (e.g., sinkholes), and generally flows northward toward the Atlantic Ocean. Discharge is principally toward wells, coastal wetlands and streams (Renken, et al., 2002). This pattern can be observed in the head vector distribution (Figure 6-1), which represents the groundwater flow direction in the area. In the western and central parts of the study area, flow tends to be northward toward the coastal zone and wetlands. Toward the eastern side, groundwater tends to flow eastward toward the Rio La Plata and toward the coast.

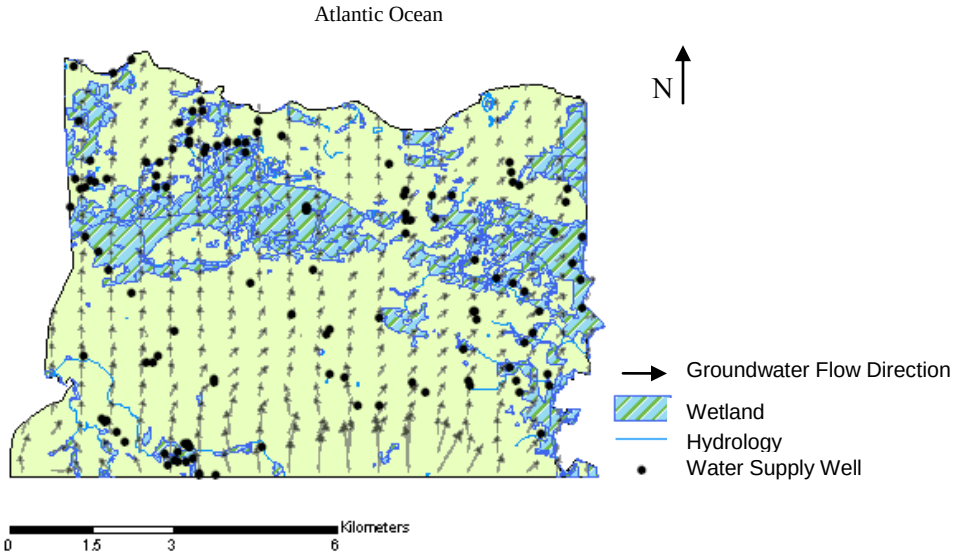

Figure 6-1: Hydraulic head vector distribution

Any contamination entering this system tends to follow the groundwater vector path, assuming that the system behaves as an equivalent porous media. The extent of contamination is influenced by the velocity of the groundwater and lateral dispersion processes. The extent of contamination delineated for a release occurring at the Vega Alta Public Water Supply Well superfund site and the CGE facility show that contaminants move toward wetlands and the coastal zone (Figure 6-2). The precise path depends on the actual location of the release. In the case that the release occurs in an area between the superfund site and CGE facility the extent would encompass the whole area delineated by both point releases (shown in the dash overlapped in Figure 6-2).

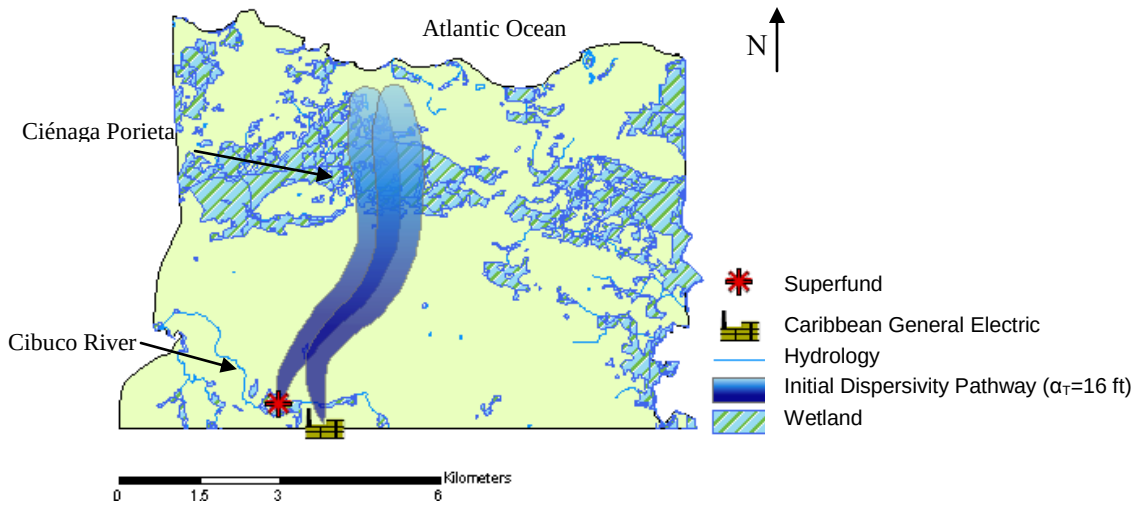

Figure 6-2: Contamination pathways from Vega Alta Water Supply superfund site and CGE; α_T=16 ft

The direction of the contamination plume is likely to go toward the northeast-north area (Figure 6-3b) in accordance to Sepúlveda (1999) report, in which the overall movement of the plume was toward the northeast at altitudes above -125ft (Figure 6-3a). In Sepúlveda's report the plume wasn't delineated up to near the coast as in this study.

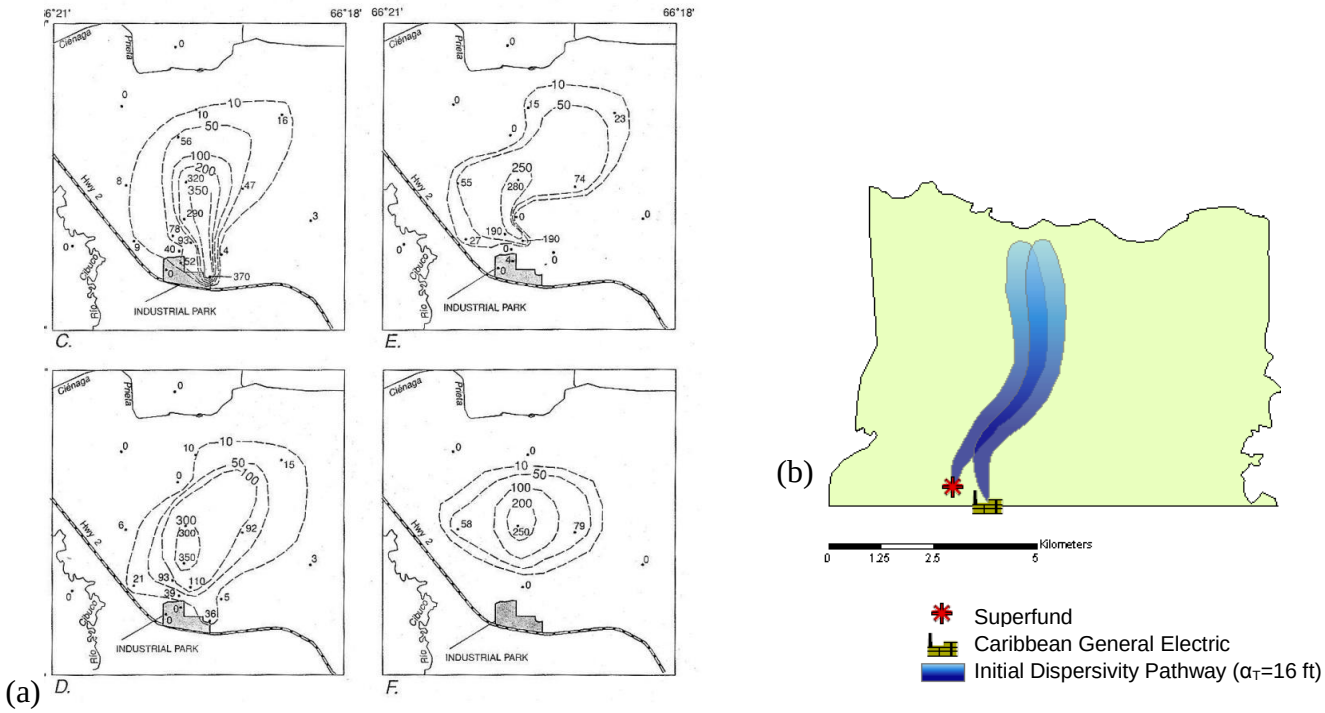

Figure 6-3 Approximate extent of TCE plume at different aquifer altitudes (a) and delineated pathways with initial dispersivity (α_T = 16ft) from superfund ID location and CGE (b) in Vega Alta – Dorado study area.

The lateral extent of contamination from the longitudinal path depends on the dispersivity value applied to the system. The pathway delineated with the maximum dispersivity value (α_T = 52 ft) has a wider extent that with the minimum dispersivity (α_T = 0.5 ft) shows a much thinner extent (Figure 6-4).

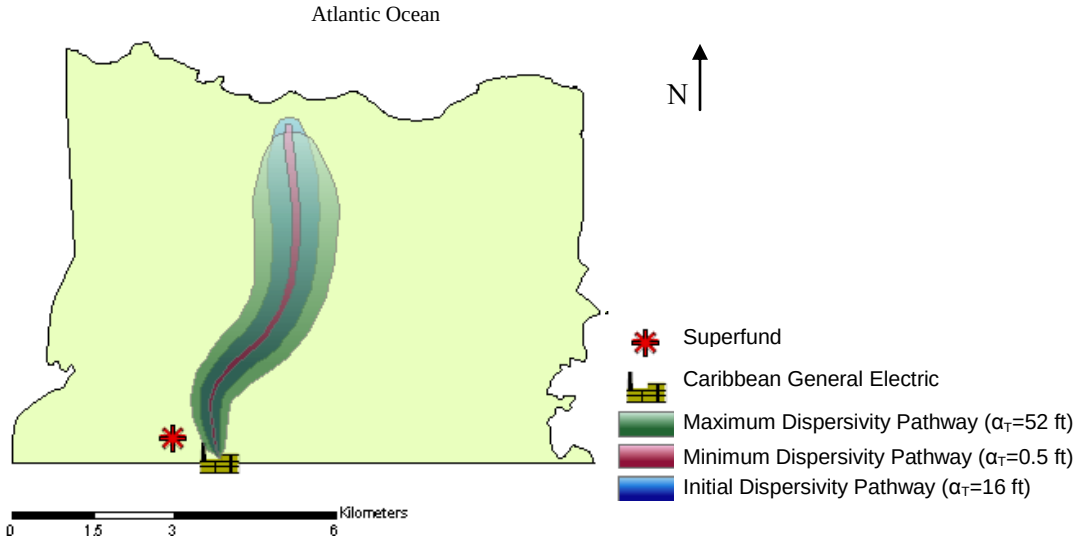

Figure 6-4: Comparison of contamination pathway from CGE for different dispersivity values (maximum α_T=52 ft; minimum α_T=0.5 ft; initial α_T=16 ft)

The use of scale-dependent dispersivity generally generates a greater extent of contamination away from the source than the use of constant dispersivity values. Near the source, the extent tends to be greater for systems with constant dispersivity. Figure 6-5 shows the contamination extent delineated with a scale dependent dispersivity in contrast with another delineated with a constant dispersivity. Near the source, the system with constant dispersivity is wider than the scale dependent dispersivity. At greater distances the extents becomes larger for the system with scale-dependent dispersivity, the same way as dispersivity increase with distance (Appelo and Postma, 2005). Similar extents are shown between the system having a maximum constant dispersivity and that having a scale-dependent dispersivity (Figure 6-6).

A map illustrating the estimated extent of contamination from superfund site and CGE facility and the wells with VOC detection (Figure 6-7), specifically with TCE, shows that some contaminated wells are within the extent of contamination. The number of wells inside the contamination extent and the range of concentration measured within the extent depend on the source location and the dispersivity values used (Table 6-1).

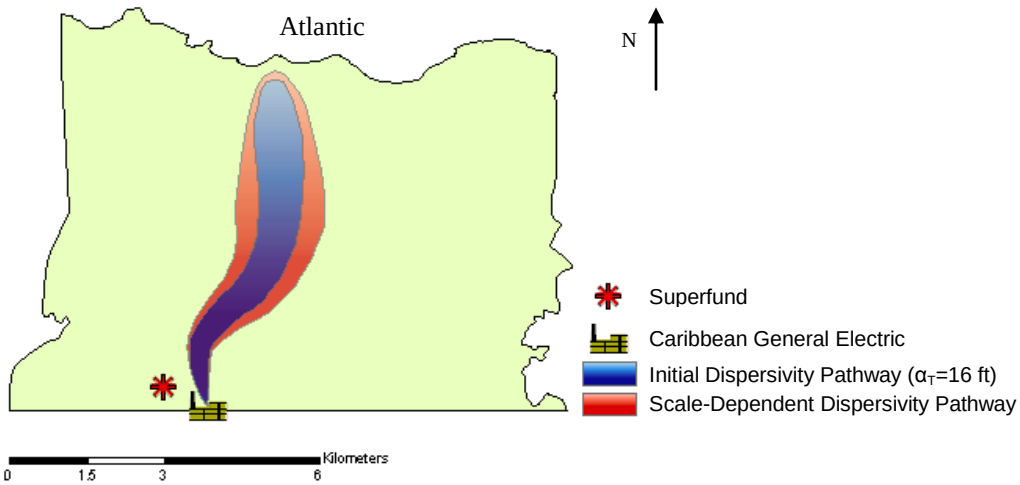

Figure 6-5: Contamination pathway from CGE for α_T=16 ft and scale-dependent dispersivity

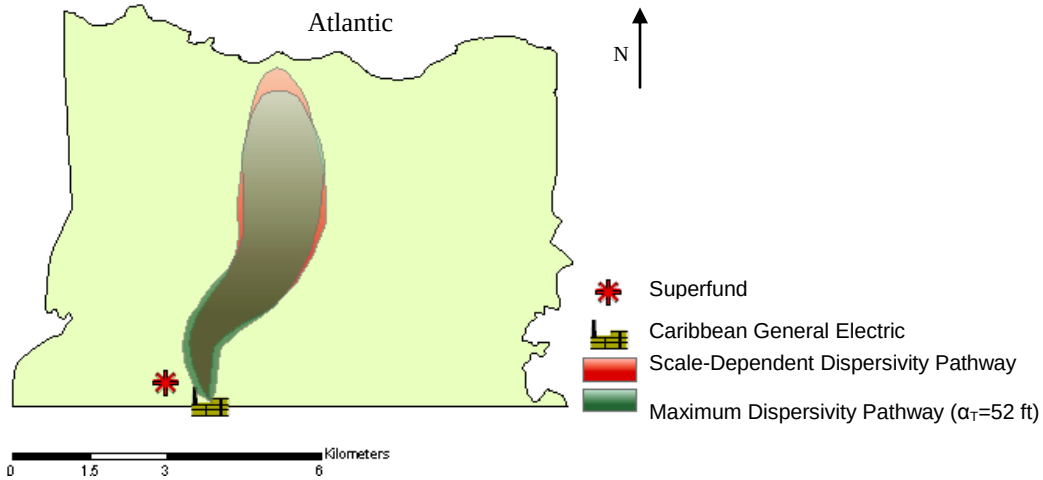

Figure 6-6: Contamination pathway for α_T=52 ft and scale-dependent dispersivity

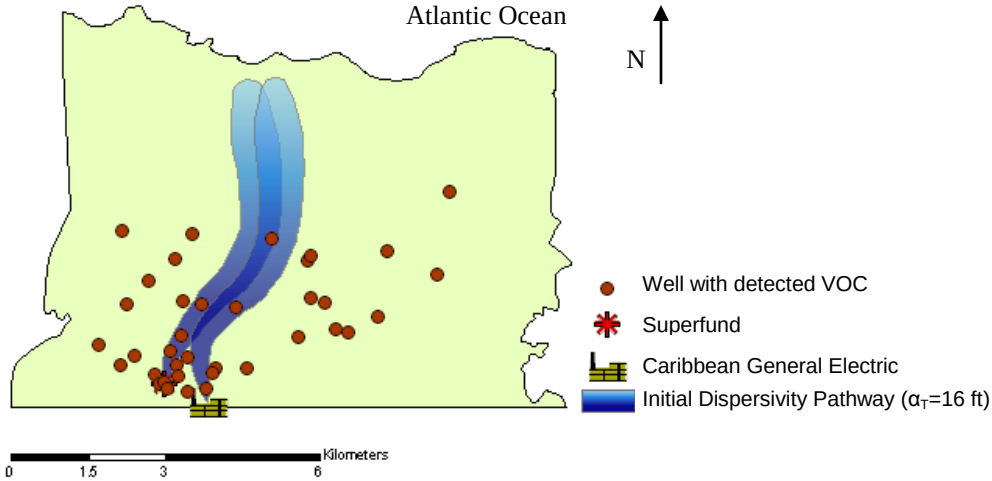

Figure 6-7: VOC detected wells within area of study in relation to contamination pathway

Table 6-1: Number and concentration range of TCE in wells within contaminant extent

Dispersivity	*# wells*	*Concentration Range*
Source 1 (Superfund)		
α = 16 ft	5	4 – 142 μg/L
Source 2 (CGE)		
α = 16 ft	3	9.5 – 944 μg/L
α = min=0.5 ft	1	9.5 μg/L
α = max= 52ft	7	9.5 – 944 μg/L
α = f(L)	3	9.5 – 944 μg/L
Source 1+2		
α = 16 ft	7	4 – 944 μg/L
α = min=0.5 ft	5	4 – 142 μg/L
α = max=52 ft	9	4 – 944 μg/L
α = f(L)	7	4 – 944 μg/L

Most of the wells within the contamination extents surpass the TCE maximum contaminant level of 5μg/L, permitted by the Environmental Protection Agency (EPA, 2008b). A greater number of contaminated wells are incorporated within the estimated extent for systems with higher dispersivity values and for an area source distribution (instead of point-source distribution). Although, the extent with the maximum dispersion value (Figure 6-8a) and scale-dependent (Figure 6-8b) concerns a larger area with VOC-detected wells, there is a large number of wells with VOC detection than are not covered by the estimated extent.

Comparison of the distribution of wells with VOC detection and the estimated contamination extent (Figure 6-9) suggest that the system may be characterized by a greater transverse dispersion coefficient, than assumed in this study. In part, differences arise from the uncertainty in the values of dispersivity. In field experiments, longitudinal dispersivity values in a porous media range in the order of 0.01 to 100 m; those in fissured and karstic rocks range from 10 m to 1,000 m (Hurst, 1991). Transversal dispersivity is assumed to be 1/10 to 1/100 of longitudinal

dispersivity. These can be observed in Figure 6-8a. Pathways with longitudinal dispersivity from 10 m to 170 m and transversal dispersivity between 0.5 m and 52 m. The difference in extent is significant and the quantity of water wells that are covered is also different.

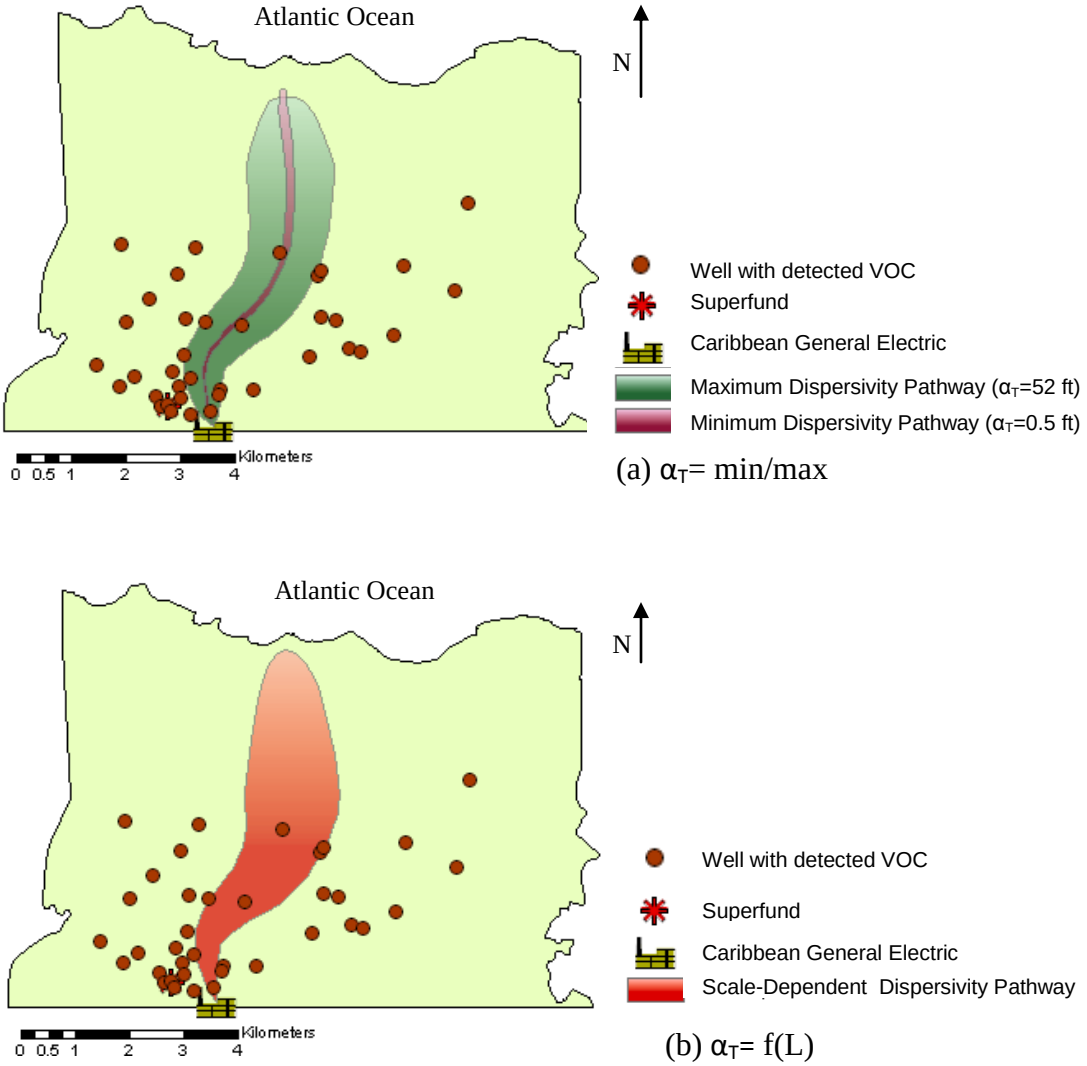

Figure 6-8: Contamination pathway with maximum/minimum (a) and scale-dependent (b) dispersivity in relation to wells with VOC detection in study area

The dispersion coefficient is a parameter used to describe dispersive transport of chemical from areas of high to low concentration. In essence this parameter describes the rate of mixing caused by variable velocity and heterogeneities (Padilla et al., 1999). The assumption that the lateral extent of contamination is mostly caused by transverse mechanical dispersion, however, does not take into account mixing processes resulting from variable temporal velocity vectors

(magnitude and direction). In karst aquifers, contaminants entering the system are subjected to multiple events of rapid mobilization during conduit storm flow followed by slower diffuse flow during baseflow conditions (Padilla and Steele, 2008). Over time, variable flow regimes cause significant dispersion of contaminants in the aquifer, extending the zones of potential exposure. Therefore, a temporal analysis must be considered when assessing the extent of contamination. Another potential source of error in the analysis presented here is the assumption that the aquifer behaves as an equivalent porous media, although several models developed for the areas (Torres-González, 1999; Cherry, 2001) have assumed porous media behavior at the regional level. Conduit flow could influence the transport and extent of contaminants in the karst aquifer.

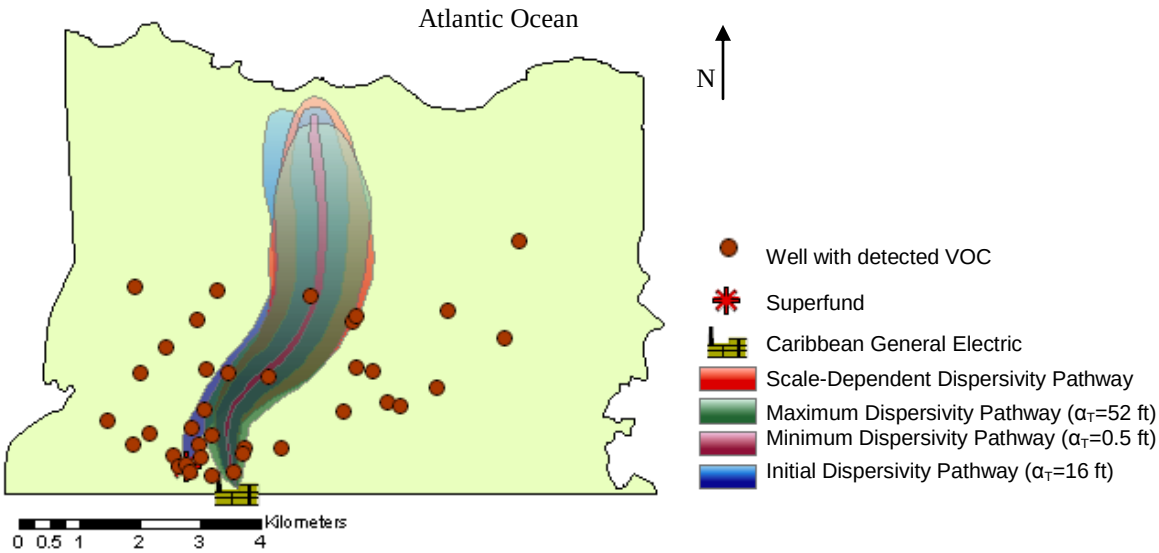

Figure 6-9: Estimated contamination pathway using different dispersivity values in relation to wells with VOC detection.

Additional differences between the estimated extents of contamination and the number of wells with VOC detection may arise from other potential sources of contamination. The numbers of sites in the study area listed by the EPA toxic release inventory (EPA 2010c) are shown in Figure 6-10. These industries are potential sources of contamination. Dry cleaners are not included here, but they are other kind of potential sources of chlorinated solvents.

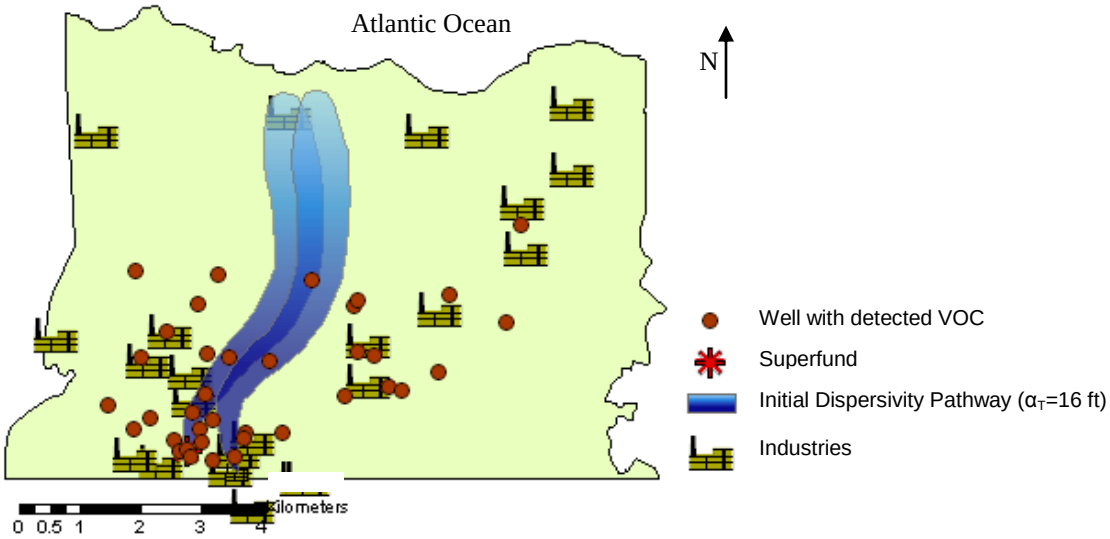

Figure 6-10: Industries in the study area in relation to wells with VOC detection in study area

Potential Groundwater Exposure

Potential exposure of contaminated groundwater could result from using water extracted from groundwater wells. Potential exposure may also occur through ingestion of food (cattle, poultry, vegetable) produced near stream and wetland areas associated with contaminated groundwater discharge. Figure 6-11 shows the extent of contamination at various dispersive properties, and the wells listed in the ground-water well inventory (PRWEI, 2007) by water use. There are several wells exist within and near the contamination extent, including: domestic and stock, public supply and industrial wells. The number of wells with potential exposure increases as the dispersive properties of the aquifer increase. The extent of contamination covers areas within the upper reaches of Rio Cibuco and the Ciénaga Porieta Wetlands.

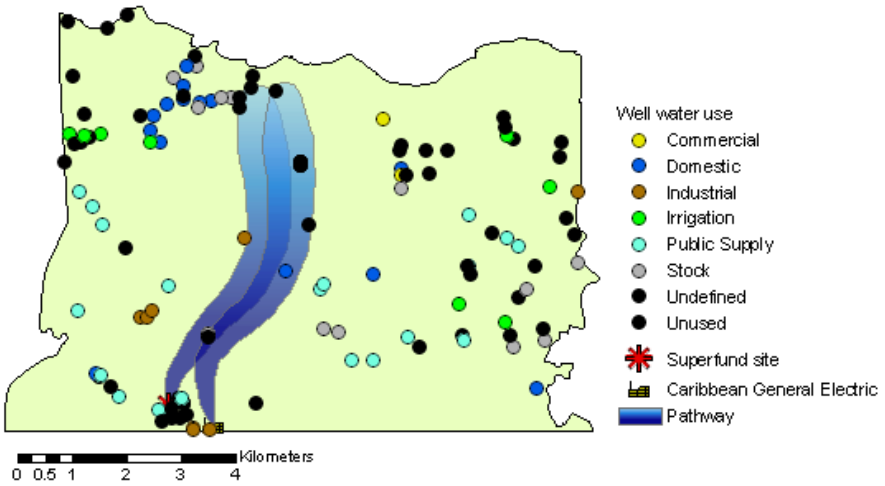

(a) α_T=16 ft

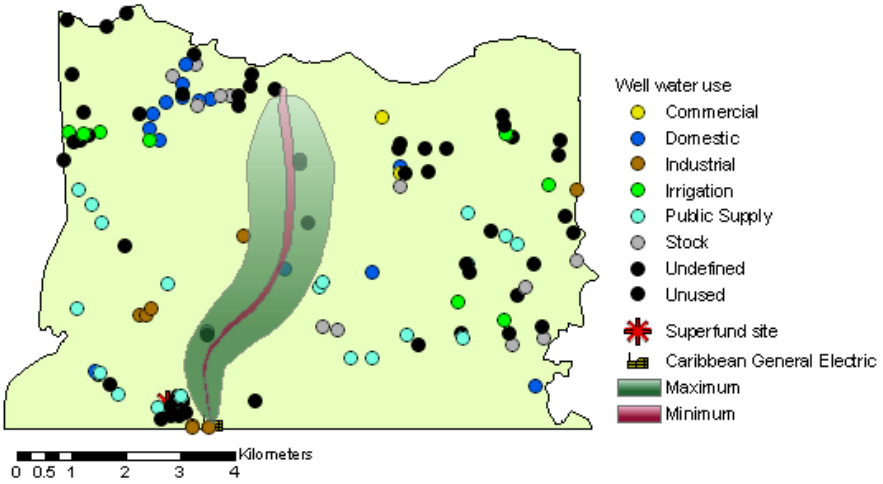

(b) α_T=max/min

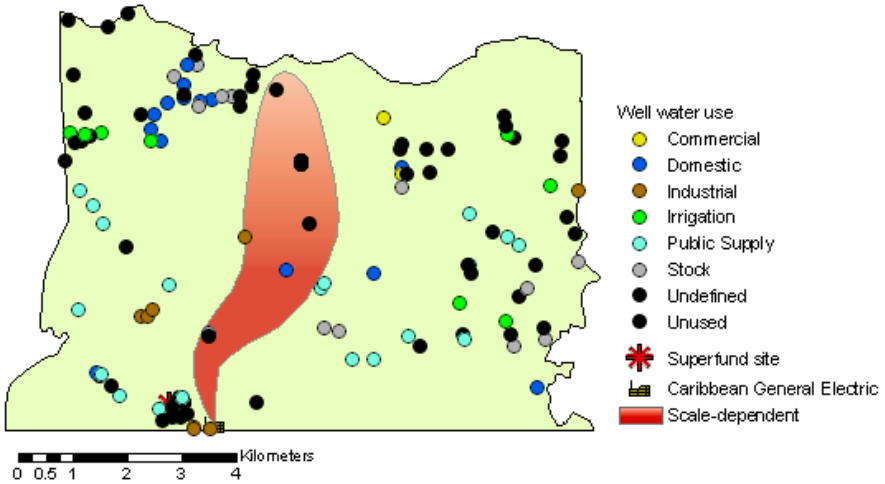

(c) α_T=f(L)

Figure 6-11: Contamination pathway with original (a) maximum/minimum (b) and scale-dependent (c) dispersivity in relation to wells with different water uses

7 Summary and Conclusions

This project assessed potential contaminant exposure pathways using geographic information system technologies. The area selected for the analysis was Vega Alta-Dorado area. Several pathways were delineated, based on advective and dispersive transport occurring from one or multiple sources. The longitudinal pathway from the source(s) was determined from steady-state hydraulic gradient vectors along the flow direction. The lateral extent was assumed to be controlled by transversal dispersion along the longitudinal pathway. The longitudinal extent of contamination extends toward the coastal zone because enough time has elapsed after the release of the contamination. The lateral extent, however, was highly sensitive to dispersivity values used in the model. In general, a constant dispersivity or linear scale-dependent dispersivity does not generate an extent of contamination that covers all wells with where VOC has been detected. However, the extents show that the contamination path could have affected domestic, public supply, industrial, and agricultural wells, as well as some streams are wetlands.

Differences between the estimated extent of contamination and the number of wells with VOC detection are attributed to: 1) a greater transverse dispersion than assumed in this study; 2) mixing and advection processes resulting from variable velocity vectors; 3) flow and transport not described by equivalent porous media; and 4) other potential sources of contamination. A greater extent of contamination may also result due to an areal release and not point sources.

Results show that GIS technology can be used for delineation of the extent of contamination provided that reasonable assumptions made in the analysis are met. ArcGIS and Spatial Analyst extension were significant tools for the construction of the contaminant pathway for this research. They are powerful tools in the integration and visualization of existing data. Information that normally would be difficult (if not impossible) to overlay, can be done easily in GIS. A large number of data are accessible and already digitized. This is of great help when modeling, because it saves time and money. It allows rapid integration of new data and avoids tedious, error-prone text editing of model input files (Watkins et al., 1996). A geographic information system helps in the visualization of potential exposure and it may assists decision-makers when a contaminant release occurs.

8 Recommendations

The reliability of the potential extent of contamination depends on the simplifying assumptions made. It is likely that variable flow conditions prevail in the system and that this variability needs to be integrated in the system. A temporal analysis must be considered when assessing the extent of contamination. The study assumed steady-state condition, so an unsteady-state me be analyzed and integrate it in the study. An equivalent porous media may not be a good representation of the system. The use of other models, such as pipe flow models, and input and output model may be compared with the equivalent porous media model. It is also likely that more than one contamination event has occurred; there are other potential sources of contamination that may be analyzed and tracked. To keep a sequential well sampling procedure along the wells of the region may be also included in the study. Another recommendation is to make the methodology more user-friendly. The dispersion calculation was made in excel worksheets and a program can be developed in Visual Basic or any other language supported by ArcGIS. This will make the procedure faster and with less human error.

Appendix A

To apply the Microsoft Visual Basic code developed by ESRI (Fried, 2003) to convert raster files to xyz data, several peculiarities had to be resolved. These are described below.

- The “Dim pPblock As IPixelBlock3” section of the code was modified to use IPixelBlock instead of the default IPixelBlock3 because the ArcGIS version used didn’t support IPixelBlock3.
- Layer naming. Inside ArcGIS the layer name can be changed using layer properties. This change of name takes place only inside the program, because in its respective folder in the computer it remains with the original name. When performing the operation in Microsoft Visual Basic code the program can read the new name inside ArcGIS, but when the tool look for the layer in the respective computer folder it doesn’t find it because it has the original name. To correct this it was necessary to rename the layer with the original name. Another way could be to change the original name as the desired one using ArcCatalog. This way all the files from the layer are changed with the new name. If this is not done an error is received in the code part “Set pRaster = pRWS.OpenRasterDataset(pLayer.Name). CreateDefaultRasterv”.

Appendix B

Wells with detected VOC in La Plata-Arecibo Study Area

Site Name	LAT	LON	Municipality	Contaminants	Date	Source
Sabana Hoyos 1	-66.60194	18.39222	Arecibo	Chloroform	Nov 1984 - May 1985	OFR 86-63
Sabana Hoyos 2	-66.60306	18.39750	Arecibo	Chloroform	Nov 1984 - May 1985	OFR 86-63
Sabana Hoyos 3	-66.60083	18.41111	Arecibo	Chloroform	Nov 1984 - May 1985	OFR 86-63
Jobales 1	-66.62917	18.36222	Arecibo	Chloroform	Nov 1984 - May 1985	OFR 86-63
Santana 1	-66.64778	18.44444	Arecibo	PCE, Chloroform	Nov 1984 - May 1985	OFR 86-63
Jobales 3	-66.63306	18.38000	Arecibo	Chloroform	Nov 1984 - May 1985	OFR 86-63
Sabana Hoyos 4	-66.61556	18.42000	Arecibo	Chloroform	Nov 1984 - May 1985	OFR 86-63
Ojo de Agua 1	-66.69028	18.39583	Arecibo	Chloroform	Nov 1984 - May 1985	OFR 86-63
Arecibo 4	-66.70694	18.41556	Arecibo	Chloroform	Nov 1984 - May 1985	OFR 86-63
Miraflores 2	-66.64917	18.42472	Arecibo	PCE, Chloroform	Nov 1984 - May 1985	OFR 86-63
Arecibo 3	-66.70250	18.42111	Arecibo	Chloroform	Nov 1984 - May 1985	OFR 86-63

Arecibo 5	-66.70639	18.41917	Arecibo	Chloroform	Nov 1984 - May 1985	OFR 86-63
Arecibo 7	-66.70972	18.41750	Arecibo	Chloroform	Nov 1984 - May 1985	OFR 86-63
Arecibo 6	-66.70889	18.41917	Arecibo	Chloroform	Nov 1984 - May 1985	OFR 86-63
Ojo de Agua 2	-66.68944	18.39556	Arecibo	Chloroform	Nov 1984 - May 1985	OFR 86-63
Miraflores 3	-66.64889	18.42806	Arecibo	Chloroform	Nov 1984 - May 1985	OFR 86-63
Wallcot	18.43556	-66.59972	Arecibo	TCE, PCE, 1,1,2-Thrichloroethane, Carbontetrachloride, Chloroform	6/25/1982	USGS NWIS
Master Concrete	18.44056	-66.68556	Arecibo	TCE, PCE, 1,1,2-Thrichloroethane, Carbontetrachloride, Chloroform	6/30/1982	USGS NWIS
Ias 5	-66.59028	18.43556	Arecibo	TCE, PCE, Carbontetrachloride, Chloroform	4/2/1990 4/6/1990 5/7/1990	USGS NWIS
Nycomed 1	-66.56361	18.43028	Arecibo	TCE, PCE, 1,1,2-Thrichloroethane, Carbontetrachloride, Chloroform	9/14/1995 9/26/1995 11/29/1995	USGS NWIS
Fomento	-66.64583	18.44972	Arecibo	TCE, PCE, 1,1,2-Thrichloroethane, Carbontetrachloride, Chloroform	9/17/1997	EPA STORET

Garrochales3	-66.59917	18.46028	Arecibo	TCE, PCE, 1,1,2-Thrichloroethane, Carbontetrachloride, Chloroform	9/17/1997	EPA STORET
				PCE, Chloroform, Methylene Chloride	Nov 1984 - May 1986	OFR 86-63
Matadero 4	-66.70667	18.41389	Arecibo	TCE, PCE, 1,1,2-Thrichloroethane, Carbontetrachloride, Chloroform	9/17/1997	EPA STORET
Miraflores 1	-66.64861	18.42417	Arecibo	TCE, PCE, 1,1,2-Thrichloroethane, Carbontetrachloride, Chloroform	9/17/1997	EPA STORET
				Chloroform	Nov 1984 - May 1986	OFR 86-63
Urbano 2	-66.69000	18.39444	Arecibo	TCE, PCE, 1,1,2-Thrichloroethane, Carbontetrachloride, Chloroform	10/2/1997	EPA STORET
Unkown 1	-66.60806	18.45667	Arecibo	Carbon Tetrachloride	10/16/1982	OFR 84-058
Abbott 1 Injection	-66.56806	18.43361	Barceloneta	TCE, PCE, 1,1,2-Thrichloroethane, Carbontetrachloride, Chloroform	10/14/1989	USGS NWIS

Ias 3	-66.57083	18.43278	Barceloneta	TCE, PCE, 1,1,2-Thrichloroethane, Carbontetrachloride, Chloroform	6/15/1989 6/27/1989	USGS NWIS
Cruce Dávila 1	-66.56694	18.43167	Barceloneta	TCE, PCE, 1,1,2-Thrichloroethane, Carbontetrachloride, Chloroform	9/11/1997	EPA STORET
Fortuna	-66.55222	18.44639	Barceloneta	TCE, PCE, 1,1,2-Thrichloroethane, Carbontetrachloride, Chloroform	9/11/1997	EPA STORET
Pajonal 1	-66.56333	18.38472	Barceloneta	TCE, PCE, 1,1,2-Thrichloroethane, Carbontetrachloride, Chloroform	9/11/1997	EPA STORET
Pajonal 2	-66.55250	18.38972	Barceloneta	TCE, PCE, 1,1,2-Thrichloroethane, Carbontetrachloride, Chloroform	9/11/1997	EPA STORET
Tiburones 2	-66.57861	18.43444	Barceloneta	TCE, PCE, 1,1,2-Thrichloroethane, Carbontetrachloride, Chloroform	9/11/1997	EPA STORET

Viskase 3	-66.55528	18.42722	Barceloneta	TCE, PCE, 1,1,2-Thrichloroethane, Carbontetrachloride, Chloroform	9/11/1997	EPA STORET
Barceloneta	-66.55222	18.44639	Barceloneta	PCE, Chloroform	Nov 1984 - May 1985	OFR 86-63
Vila	-66.55917	18.43194	Barceloneta	Chloroform	Nov 1984 - May 1985	OFR 86-63
Cimarrona	-66.57750	18.41167	Barceloneta	Chloroform	Nov 1984 - May 1985	OFR 86-63
Unkown 2	-66.58917	18.43556	Barceloneta	Carbon Tetrachloride	7/18/1983	OFR 84-058
Coto Norte 3	-66.45972	18.44139	Manatí	TCE, PCE, 1,1,2-Thrichloroethane, Carbontetrachloride, Chloroform	9/11/1997	EPA STORET
Manatí 2	-66.50139	18.42944	Manatí	TCE, PCE, 1,1,2-Thrichloroethane, Carbontetrachloride, Chloroform	9/11/1997	EPA STORET
				Methylene Chloride	Nov 1984 - May 1986	OFR 86-63
Monserrate Sur	-66.49694	18.40333	Manatí	TCE, PCE, 1,1,2-Thrichloroethane, Carbontetrachloride, Chloroform	9/11/1997	EPA STORET

Ias 1	-66.47028	18.45889	Manati	TCE, PCE, 1,1,2-Thrichloroethane, Carbontetrachloride, Chloroform	1/16/1990	USGS NWIS
Coto Norte 2	-66.44306	18.44167	Manatí	Chloroform, Methylene Chloride	Nov 1984 - May 1985	OFR 86-63
Coto Sur 2	-66.44639	18.43111	Manatí	Chloroform	Nov 1984 - May 1985	OFR 86-63
Manatí 3	-66.49028	18.43444	Manatí	TCE, PCE, Chloroform	Nov 1984 - May 1985	OFR 86-63
Rio Arriba 3	-66.46361	18.38667	Manatí	Chloroform	Nov 1984 - May 1985	OFR 86-63
Coto Sur 1	-66.46500	18.42778	Manatí	Chloroform, Methylene Chloride	Nov 1984 - May 1985	OFR 86-63
Monaco	-66.48361	18.42056	Manatí	Chloroform, Methylene Chloride	Nov 1984 - May 1985	OFR 86-63
Rabanos	-66.49000	18.45389	Manatí	TCE, PCE, Chloroform, Methylene Chloride	Nov 1984 - May 1985	OFR 86-63
Boquilla	-66.49361	18.46417	Manatí	Chloroform, Methylene Chloride	Nov 1984 - May 1985	OFR 86-63
Manati 1	-66.50056	18.43028	Manatí	Methylene Chloride	Nov 1984 - May 1985	OFR 86-63
Montebello 2	-66.52222	18.37194	Manatí	Chloroform	Nov 1984 - May 1985	OFR 86-63
Montebello 5	-66.52889	18.36972	Manatí	Chloroform	Nov 1984 - May 1985	OFR 86-63
Unkown 3	-66.49167	18.43333	Manatí	TCE, PCE	1983	OFR 85-810

Pugnado 3	-66.43833	18.43056	Vega Baja	TCE, PCE, 1,1,2-Thrichloroethane, Chloroform	10/24/1988	USGS NWIS
				PCE, Chloroform	Nov 1984 - May 1985	OFR 86-63
Almirante 2	-66.36861	18.41444	Vega Baja	Chloroform	Nov 1984 - May 1985	OFR 86-63
Almirante 3	-66.37250	18.43306	Vega Baja	Chloroform	Nov 1984 - May 1985	OFR 86-63
Criollo 1			Vega Baja	Chloroform	Nov 1984 - May 1985	OFR 86-63
Vega Baja 3	-66.40139	18.44556	Vega Baja	TCE, PCE, Chloroform	Nov 1984 - May 1985	OFR 86-63
Criollo 2			Vega Baja	TCE, PCE, Chloroform, Methylene Chloride	Nov 1984 - May 1985	OFR 86-63
Urb. Altura			Vega Baja	PCE, Chloroform	Nov 1984 - May 1985	OFR 86-63
Pugnado 1	-66.40806	18.43139	Vega Baja	PCE, Chloroform	Nov 1984 - May 1985	OFR 86-63
Pugnado 2	-66.41056	18.42917	Vega Baja	PCE	Nov 1984 - May 1985	OFR 86-63
Sobrino	-66.43250	18.43861	Vega Baja	Chloroform	Nov 1984 - May 1985	OFR 86-63
Unkown 4	-66.45889	18.43972	Vega Baja	Methylene Chloride	June-July 1982	OFR 84-058
Bechtel 16	-66.33806	18.44500	Vega Alta	TCE	March 1992	USGS WRI 97-4170
Bechtel 5	-66.32528	18.44444	Vega Alta	TCE	March 1992	USGS WRI 97-4170

Bechtel 17	-66.31056	18.44361	Vega Alta	TCE	January 1990 March 1992	USGS WRI 97-4170
Bechtel 2	-66.32833	18.44000	Vega Alta	TCE	March 1992	USGS WRI 97-4170
Forestal Marismina	-66.30389	18.43972	Vega Alta	TCE	March 1992	USGS WRI 97-4170
Los Puertos	-66.30333	18.44056	Vega Alta	TCE	March 1992	USGS WRI 97-4170
Gramas Lindas 2	-66.28000	18.43722	Vega Alta	TCE	March 1992	USGS WRI 97-4170
El Morro Corrugated	-66.33333	18.43611	Vega Alta	TCE	March 1992	USGS WRI 97-4170
Bechtel 9	-66.32694	18.43278	Vega Alta	TCE	March 1992	USGS WRI 97-4170
Monterrey 1	-66.30333	18.43306	Vega Alta	TCE	March 1992	USGS WRI 97-4170
Reyes	-66.30083	18.43250	Vega Alta	TCE	January 1990 March 1992	USGS WRI 97-4170
Bechtel 4	-66.33722	18.43222	Vega Alta	TCE	March 1992	USGS WRI 97-4170
Monterrey 2	-66.32361	18.43222	Vega Alta	TCE	March 1992	USGS WRI 97-4170
Bechtel 8	-66.31722	18.43167	Vega Alta	TCE	March 1992	USGS WRI 97-4170
Maguayo 2	-66.29861	18.42778	Vega Alta	TCE	March 1992	USGS WRI 97-4170
				TCE, PCE, Chloroform	Nov 1984 - May 1985	OFR 86-63

Maguayo 3	-66.29639	18.42722	Vega Alta	TCE	March 1992	USGS WRI 97-4170
Bechtel 3	-66.32722	18.42667	Vega Alta	TCE	March 1992	USGS WRI 97-4170
Bechtel 13	-66.30556	18.42639	Vega Alta	TCE	January 1990 March 1992	USGS WRI 97-4170
Bajura 5	-66.34250	18.42500	Vega Alta	TCE	March 1992	USGS WRI 97-4170
				TCE, PCE	Nov 1984 - May 1985	OFR 86-63
Bechtel 11	-66.32917	18.42389	Vega Alta	TCE	March 1992	USGS WRI 97-4170
Bechtel 10	-66.33583	18.42306	Vega Alta	TCE	March 1992	USGS WRI 97-4170
Bechtel 12	-66.32611	18.42278	Vega Alta	TCE	March 1992	USGS WRI 97-4170
Bajura 1	-66.33861	18.42139	Vega Alta	TCE	March 1992	USGS WRI 97-4170
Bechtel 6	-66.32806	18.42139	Vega Alta	TCE	March 1992	USGS WRI 97-4170
Bechtel 19	-66.32083	18.42083	Vega Alta	TCE	March 1992	USGS WRI 97-4170
Santa Ana	-66.31528	18.42083	Vega Alta	TCE	January 1990 March 1992	USGS WRI 97-4170
Alta Nursery	-66.32139	18.42000	Vega Alta	TCE	March 1992	USGS WRI 97-4170
GE 2 (Bajura 4)	-66.33222	18.41972	Vega Alta	TCE	January 1990 March 1992	USGS WRI 97-4170

Bechtel 14	-66.32778	18.41944	Vega Alta	TCE	January 1990 March 1992	USGS WRI 97-4170
Bechtel 1	-66.33028	18.41833	Vega Alta	TCE	January 1990 March 1992	USGS WRI 97-4170
Harman 1	-66.32972	18.41722	Vega Alta	TCE	January 1990 March 1992	USGS WRI 97-4170
Bechtel 22	-66.32278	18.41722	Vega Alta	TCE	January 1990 March 1992	USGS WRI 97-4170
Levi 1	-66.32611	18.41667	Vega Alta	TCE	January 1990 March 1992	USGS WRI 97-4170
Ponderosa (Out)	-66.32806	18.42139	Vega Alta	TCE, PCE, 1,1,2-Thrichloroethane, Carbontetrachloride, Chloroform	3/3/1986 3/4/1986 3/5/1986 3/6/1986 3/7/1986 10/26/1989	USGS NWIS
Vega Alta 1	-66.33000	18.41278	Vega Alta	TCE, PCE, Chloroform	Nov 1984 - May 1985	OFR 86-63
Regadera	-66.33083	18.43972	Vega Alta	TCE, PCE, Chloroform, Methylene Chloride	Nov 1984 - May 1985	OFR 86-63
Vega Alta 2	-66.33000	18.41250	Vega Alta	TCE, PCE, Chloroform	Nov 1984 - May 1985	OFR 86-63
Sabana Hoyos 3	-66.35278	18.44833	Vega Alta	Chloroform	Nov 1984 - May 1985	OFR 86-63
Unkown 5	-66.30444	18.43972	Vega Alta	TCE, PCE	1983	OFR 84-810
Unkown 6	-66.32361	18.43139	Vega Alta	TCE, PCE	1983	OFR 84-810

Unkown 7	-66.32972	18.41306	Vega Alta	TCE, PCE	1983	OFR 84-810
Unkown 8	-66.33083	18.41861	Vega Alta	TCE, PCE	1983	OFR 84-810
Unkown 9	-66.33194	18.43889	Vega Alta	TCE, PCE	1983	OFR 84-810
Unkown 10	-66.33861	18.42139	Vega Alta	TCE, PCE	1983	OFR 84-810
Unkown 11	-66.34250	18.42500	Vega Alta	TCE, PCE	1983	OFR 84-810
Unkown 12	-66.32778	18.4208333	Vega Alta	TCE, PCE	June-July 1982	OFR 84-058
Unkown 13	-66.33000	18.41278	Vega Alta	TCE	1/18/1983	OFR 84-058
Unkown 14	-66.32361	18.43222	Vega Alta	TCE	3/9/1983	OFR 84-058
Unkown 15	-66.33333	18.43611	Vega Alta	TCE	3/8/1983	OFR 84-058
Maguayo 4	-66.29083	18.43000	Dorado	PCE, Carbontetrachloride, Chloroform	9/17/1997	EPA STORET
San Antonio 2	-66.27778	18.45194	Dorado	TCE, PCE, 1,1,2-Thrichloroethane, Carbontetrachloride, Chloroform	9/17/1997	EPA STORET
Higuillar 1	-66.27833	18.44333	Dorado	TCE, PCE, Chloroform, Methylene Chloride	Nov 1984 - May 1985	OFR 86-63
Vivoni	18.39000	-66.31639	Dorado	PCE, Chloroform	Nov 1984 - May 1985	OFR 86-63
Maguayo 3	-66.29639	18.42722	Dorado	TCE, PCE, Chloroform, Methylene Chloride	Nov 1984 - May 1985	OFR 86-63

San Antonio 3	-66.26944	18.44667	Dorado	PCE	Nov 1984 - May 1985	OFR 86-63
Unkown 16	-66.27806	18.4433333	Dorado	1,2-trans-dichloroethylene	June-July 1982 3/8/1983	OFR 84-058
Campanilla 8	-66.22222	18.42528	Toa Baja	Chloroform	Nov 1984 - May 1985	OFR 86-63
Campanilla 7	-66.22833	18.42556	Toa Baja	Chloroform	Nov 1984 - May 1985	OFR 86-63
Campanilla 6	-66.23000	18.42500	Toa Baja	PCE	Nov 1984 - May 1985	OFR 86-63
Unkown 17	-66.17694	18.4294444	Toa Baja	TCE, PCE	1983	OFR 84-810

Reference

Agency for Toxic Substances and Disease Registry (ATSDR). (1997, September). Toxicological Profile for Trichloroethylene (TCE). Last accessed May 15, 2011 http://www.atsdr.cdc.gov/ToxProfiles/tp19.pdf

Agency for Toxic Substances and Disease Registry (ATSDR). (2005, September). Public Health Assessment for Pesticide Warehouse III. Last accessed July 2, 2010 http://www.atsdr.cdc.gov/hac/pha/pesticidewarehouseiii/pesticidewarehousepha090905.pdf.

Agency for Toxic Substances and Disease Registry (ATSDR). (n.d). ATSDR Glossary of Terms. Last accessed July 2, 2010. http://www.atsdr.cdc.gov/glossary.html.

Antonakos, A.K. and Lambrakis,N.J. (2007). Development and Testing of Three Hybrid Methods for the Assessment of Aquifer Vulnerability to Nitrates, Based on the Drastic Model, an Example from NE Korinthia, Greece, *Journal of Hydrology*, 333(2-4), 288-304.

Appelo, C.A.J. and Postma, D. (2005). *Geochemistry, groundwater and pollution*. Amsterdam: A.A. Balkema Publishers.

Babiker, I.S., Mohamed M.A., Hiyama, T., Kato, K. (2005). A GIS-based DRASTIC model for assessing aquifer vulnerability in Kakamigahara Heights, Gifu Prefecture, central Japan. *Science of the Total Environment*, 345(1-3), 127– 140.

Bajarska, K., Bzowski Z., and Dawidowski A. (2004). Application of GIS Elements in Underground water monitoring in the Region of Municipal Wastes Dump, *10th EC GI & GIS Workshop*. 23-25 June, 2004. Warsaw. Last accessed July 2, 2010 http://www.ec-gis.org/Workshops/10ec-gis/papers/poster_bojarska.pdf.

Batu, V. (2006). *Applied Flow and Solute Transport Modeling in Aquifers: Fundamental Principles and Analytical and Numerical Methods*. Boca Raton: Taylor & Francis Group, LLC.

Bauer M.J. and Herrmann R., (1998)**,** Dissolved Organic Carbon as the Main Carrier of Phthalic Acid Esters in Municipal Landfill Leachates, *Waste Management & Research*, 16 (5), 446-454.

Census Bureau. (2000). Oficina del Censo: Perfil Demográfico por Municipio, Censo 2000. Last accessed July 2, 2010. http://www.censo.gobierno.pr/.

Cherry, G.S. (2001). *Simulation of Flow in the Upper North Coast Limestone Aquifer, Manatí-Vega Baja Area, Puerto Rico.* (WRI 00-4266). U.S. Geological Survey: Water Resource Division.

Dassargues, A. and Derouane, J. (1998). A modelling approach as an intermediate step for the study of protection zones in karstified limestones. In: *Karst Hydrology,* Proceedings of Rabat Workshop W2, IAHS Publication 247, 71-79.

Delleur, J. (1999). *Handbook of Groundwater Engineering*.Boca Raton: CRC Press LLC.

Department of Natural and Environmental Resources (DRNA). (2008). Capítulo 5: Balance de Disponibilidad Regional [Electronic version]. *Plan Integral de Recursos de Agua de Puerto Rico*. Last accessed January 13, 2011. http://www.drna.gobierno.pr/oficinas/arn/agua/negociadoagua/planagua/plan-integral-de-recursos-de-agua-de-puerto-rico/plan-integral-de-recursos-de-agua-de-puerto-rico-2008/

Department of Natural and Environmental Resources (DRNA). (2005). Capítulo 2: Clima [Electronic version]. *Inventario de Recursos de Agua de Puerto Rico (Borrador)*. Last accessed January 13, 2011 http://www.drna.gobierno.pr/oficinas/arn/agua/negociadoagua/planagua/inventario-recursos-de-agua/inventario-de-recursos-de-agua-de-puerto-rico/

Dixon, B. (2005). Applicability of Neuro-Fuzzy Techniques in Predicting Ground-Water Vulnerability: a GIS-Based Sensitivity Analysis, *Journal of Hydrology,* 309(1-4), 17-38.

Environmental Protection Agency (EPA). (1987a). EPA Superfund Record of Decision: Vega Alta Public Supply Wells [Electronic version]. EPA/ROD/R02-87/050.

Environmental Protection Agency (EPA). (1987b). DRASTIC: A standardized system for evaluating ground water pollution potential using hydrogeologic settings. EPA/600/2-87/035

Environmental Protection Agency (EPA). (1988). EPA Superfund Record of Decision: Uphohn Facility [Electronic version]. EPA/ROD/R02-88/071.

Environmental Protection Agency (EPA). (1996). EPA Superfund Record of Decision: Barceloneta Landfill [Electronic version]. EPA/ROD/R02-96/284.

Environmental Protection Agency (EPA). (1999). Five-Year Review Report, Vega Alta Public Supply Wells Superfund Site, Vega Alta, Puerto Rico [Electronic Version].

Environmental Protection Agency (EPA). (2004). EPA Superfund Record of Decision: Vega Baja Solid Waste Disposal [Electronic version]. EPA/ROD/R2004020001421

Environmental Protection Agency (EPA). (2006a). EPA Superfund Record of Decision: Scorpio Recycling, Inc. [Electronic version]. EPA/ROD/R2006020001432

Environmental Protection Agency (EPA). (2006b). EPA Says More Landfills in Puerto Rico Must Be Addressed. Last accessed July 2, 2010 http://yosemite.epa.gov/opa/admpress.nsf/b6f538027a6b8c37852572a000650c04/cd3e8ea00ad81f7e852571cb0055580d!OpenDocument.

Environmental Protection Agency (EPA). (2008a). STORET Database Access. Last accessed July 2, 2010. http://www.epa.gov/storpubl/dbtop.html.

Environmental Protection Agency (EPA). (2008b). Drinking Water Contaminants, Last accessed July 2, 2010. http://www.epa.gov/ogwdw000/contaminants/index.html.

Environmental Protection Agency (EPA). (2008c). Pesticide Warehouse I. Last accessed June 30, 2010. http://www.epa.gov/Region2/superfund/npl/0202985c.pdf.

Environmental Protection Agency (EPA). (2010a). Final National Priorities List (NPL) Sites - by State. Last accessed June 30, 2010. http://www.epa.gov/superfund/sites/query/queryhtm/nplfin.htm#PR.

Environmental Protection Agency (EPA). (2010b). Deleted National Priorities List (NPL) Sites - by State. Last accessed June 30, 2010 http://www.epa.gov/superfund/sites/query/queryhtm/npldel.htm#PR.

Environmental Protection Agency (EPA). (2010c). TRI Explorer – Facility report. Last accessed June 30, 2010. http://www.epa.gov/triexplorer/facility.htm.

ESRI. (2001). *Using ArcGIS Spatial Analyst*. Redlands: ESRI.

ESRI. (2003). Computer Program ArcGIS® 8.3. http://www.esri.com/software/arcgis/index.html

Fetter, C.W. (1999). *Contaminant Hydrogeology* (2nd edition). Upper Saddle River: Prentice-Hall, Inc.

Field, M. (1999). Quantitable analysis of tracer breakthrough curves from tracing test in karst aquifers, in Proceedings of *Karst Modeling*, February 24-27, 1999, Charlottesville, VA.

Florida Department of Health (FDH). (2003). Assessing Risk to Public Health from Petroleum Contamination in Potable Wells Using Geographic Information Systems. Bureau of Water Programs, SUPER Act.

Ford, D.C. and Williams P. (2007). *Karst, Hydrogeology & Geomorphology*. England: John Wiley & Sons.

Fried C., (2003). Computer program: Import/Export Zmap ASCII Grid to Arc Grid v2.6. Last accessed July 1, 2010. http://arcscripts.esri.com/details.asp?dbid=13093.

Gelhar, L.W., Gutjahr A.L., and Naff, R.L. (1979). Stochastic analysis of macrodispersion in a stratified aquifer, *Water Resources Research*, 15, 1387-1397

Geophysics Study Committee, Geophysics Research forum, Commission on Physical Sciences (GSC), Mathematics, and Resources, and National Research Council. (1984). *Groundwater Contamination*. Washington, DC: National Academy Press.

Giusti, E.V. and Bennett, G.D. (1976). *Water Resources of the North Coast Limestone Area, Puerto Rico.* (WRI 42-75). US Geological Survey: Water Resource Division.

Golden Software. (2008). Surfer® Version 8.09. http://www.goldensoftware.com/

Goldscheider, N. and Drew, D. (2007). *Methods in Karst Hydrogeology*. New York: Taylor & Francis

Göppert, N. and Goldscheider, N. (2008). Solute and Colloid Transport in Karst Conduits under Low- and High-Flow Conditions, *Ground Water,* 46(1), 61-68.

Guzman-Rios, S. and Quiñones, F. (1984). Ground-water quality at selected sites throughout Puerto Rico, September 1982-July 1983. (OFR 84-58). US Geological Survey.

Guzmán-Rios, S. and Quiñones-Márquez, F. (1985) Reconnaissance of trace-organic compounds in ground water throughout Puerto Rico, October 1983, (OFR 84-810). US Geological Survey.

Guzmán-Ríos, S., García, R. and Avilés, A. (1986)**.** Reconnaissance of Volatile Synthetic Organic Chemicals at Public Water Supply Wells thopughout Puerto Rico. (OFR 86-63). U.S. Geological Survey.

Ha, E., Cho, S.I., Chen, D., Chen, C., Ryan, L., Smith, T.J., Xu, X. and Christiani. D.C. (2002). Parental Exposure to Organic Solvents and Reduced Birth Weight. *Archives of Environmental Health*, 57(3), 207-214.

Hargrove, W.W., Levine, D.A., Miller, M.R., Coleman, P.R., Pack, D.L. and Durfee, R.C. (1996). GIS and Risk Assessment: A Fruitful Combination. *Proceedings of the Sixteenth Annual ESRI User Conference*. Last accessed July 2, 2010. http://proceedings.esri.com/library/userconf/proc96/to50/pap028/p28.htm

Harris, S.J. (1997). Evaluating Possible Human Exposure Pathways to Populations Relative to Hazardous Materials Sites. *Proceedings of the Seventheen Annual ESRI User Conference.* Last accessed July 2, 2010. http://proceedings.esri.com/library/userconf/proc97/proc97/to450/pap409/p409.htm.

Hassan, M.M., Atkins, P.J., and Dunn, C.E. (2003). The Spatial Pattern of Risk from Arsenic Poisoning: A Bangladesh Case Study. *Journal of Environmental Science and Health*, A38(1), 1–24.

Hillier, F.S. and Lieberman, G.J. (2001). *Introduction to operations research.* New York: McGraw-Hill.

Hurst, C.J. (1991). *Modeling the environmental fate of microorganisms*. Washington, DC: American Society of Microbiology.

Hunter, J.M. and Arbona, S.I. (1995). Paradise Lost: An Introduction to the Geography of Water Pollution in Puerto Rico. *Social Science and Medicine*, 40(10), 1331-1355.

Kamilova, E., Fayzieva, D., Nurtaev , B., Oelovsky , L. and Reible, D. (2007). GIS Use in The Aral Sea Aral Water Quality and Population's Health, in *Information Technologies in Environmental Engineering*, ITEE 2007 - Third International ICSC Symposium, 497-508.

Kelsey, H., Porter, D.E., Scott, G., Neet, M. and White, D. (2004), Using Geographic Information Systems and Regression Analysis to Evaluate Relationships between Land Use and Fecal Coliform Bacterial Pollution. *Journal of Experimental Marine Biology and Ecology*, 298(2), 197-209.

Khattak, S. (1999). Pregnancy Outcome Following Gestational Exposure to Organic Solvents: a Prospective Controlled Study. *JAMA*, 281(12), 1106-1109

Latini, G., De Felice, C., Presta, G., Del Vecchio, A., Paris, I., Ruggieri, F., and Mazzeo, P. (2003). In Utero Exposure to Di-(2-Ethylhexyl)Phthalate and Duration of Human Pregnancy. *Environmental Health Perspectives*, 111(14), 1783-1785.

Leibundgut C., Gunn, J. and Dassargues, A. (1998). *Karst Hydrology*. Publication No. 247. UK: IAHS Press.

Lipscomb, J. A. and Fenster, L. (1991). Pregnancy Outcomes in Women Potentially Exposed to Occupational Solvents and Women Working in the Electronics Industry. *Journal of Occupational Medicine*, 33(5), 597-604.

Loop, C.M. and White, W.B. (2001). A Conceptual Model for DNAPL Transport in Karst Groundwater Basins, *Ground Water*, 39(1), 119-127.

Lucas, L. and Jauzein, M.. (2008). Use of principal component analysis to profile temporal and spatial variations of chlorinated solvent concentration in groundwater. *Environmental Pollution*, 151(1), 205-212.

March of Dimes. (2007). Nacimientos Pretérmino en Puerto Rico 1990-2004 [Visual Presentation]. Writen comunication.

Molina-Rivera, W.L. (1996a). *Ground-Water Use from the Principal Aquifers in Puerto Rico During Calendar Year 1990.* (FS 188-96). U.S. Geological Survey.

Molina-Rivera, W.L. (1996b). *Puerto Rico Water-Use Program: Public Water Use and Wastewater Disposal During 1990.* (FS 098-96). U.S. Geological Survey.

Monroe W. (1980). *Geology of the middle Tertiary formations of Puerto Rico*. (PP 953). U.S. Geological Survey.

National Institute of Health. (2006). *NTP-CERHR Monograph on the potential human reproductive and Development Effects of Di(2-Ethylhexyl) Phthalate (DEHP).* (NIH Publication No. 06-4476).

National Research Council (NRC). (2005). *Contaminants in the Subsurface: Source Zone Assessment and Remediation*, Washington, D.C: The National Academies Press.

Nobre, R.C.M., Rotunno, O.C., Filho, Mansur, W.J., Nobre, M.M.M., Cosenza, C.A.N. (2007). Groundwater vulnerability and risk mapping using GIS, modeling and a fuzzy logic tool. *Journal of Contaminant Hydrology*, 94(3-4), 277–292.

Ott, R.L. and Longnecker, M. (2001). *An Introduction to Statistical Methods and Data Analysis.* (5th edition). Pacific Grove: Duxbury.

Padilla, I.Y. and Steele, K. (2008)**.** Controlling Transport Processes in Groundwater Contamination in the North Coast Aquifer of Puerto Rico. *EOS Transactions AGU*, 89(23).

Padilla I.Y., Jim Yeh, T.C and Conklin, M.H. (1999), The Effect of Water Content on Solute Transport in Unsaturated Porous Media, Department of Hydrology and Water Resources, *Water Resources Research*, 35(11), 3303–3313.

Puerto Rico Water Resource and Environmental Research Institute (PRWRERI). (2007). *GIS data*. written communication.

Puerto Rico Aqueduct and Sewer Authorithy (PRASA). (2008). *Data GIS: Infra-Agua Potable Región Norte*. Puerto Rico. written communication

Puerto Rico Planning Board (PRPB). (2008). *Data GIS: UPR datos*. written communication

Randal, T.L., Copa, W.M. and Berrigan, K.K. (1994). *Powdered Activated Carbon Treatment of Aqueous Waste at Superfund sites, in Bioremediation--field Experience.* Boca Raton: CRC press.

Renken, R.A., Ward, W.C., Gill, I.P., Gómez-Gómez, F. and Rodríguez-Martínez, J. (2002). *Geology and Hydrogeology of the Caribbean Islands Aquifer System of the Commonwealth of Puerto Rico and the U.S. Virgin Islands.* (PP 1419) U.S. Geological Survey.

Rodríguez-Martínez, J. (1994). *Hydrogeology of the North Coast Limestone Aquifer System of Puerto Rico.* (WRI 94-4249). U.S. Geological Survey: Water-Resources Investigation

Saltelli, A., Tarantola, S., Campolongo, F. and Ratto, M. (2004). *Sensitivity analysis in practice: a guide to assessing scientific models*. West Sussex: John Wiley & Sons Ltd.

Sauer, A., Schanze, J. and Walz, U. (2007), Development of a GIS-Based Risk Assessment Methodology for Flood Pollutants, *in* Information Technologies in Environmental Engineering, *ITEE 2007* – Third International ICSC Symposium, 357-366.

Schilling, K. E. and Helmers, M. (2008), Tile drainage as karst: Conduit Flow and Diffuse Flow in a Tile-Drained Watershed, *Journal of Hydrology* , 349(3-4), 291– 301.

Sepúlveda, N. (1999). *Ground-Water Flow, Solute Transport, and Simulation of Remedial Alternatives for the Water-Table Aquifer in Vega Alta, Puerto Rico*. (WRI 97-4170). U.S. Geological Survey: Water-Resources Investigations.

Thapinta, A. and Hudak, P.F. (2003). Use of geographic information systems for assessing groundwater pollution potential by pesticides in Central Thailand. *Environment International*, 29(1), 87–93.

Todd, D.K. and Mays, L.W. (2005). *Groundwater Hydrology*. (3rd edition). Hoboken: John Wiley & Sons, Inc.

Torres-González, S. (1996). *Hydrogeology and simulation of ground-water flow in the upper Aquifer of the Rio Camuy to Rio Grande de Manatí area, Puerto Rico*. (WRI 95-4286). U.S. Geological Survey: Water-Resources Investigations.

U.S. Geology Survey (USGS). (2008). Water Quality Samples for Puerto Rico [Online]. Last accessed June 30, 2010. http://nwis.waterdata.usgs.gov/pr/nwis/qwdata.

U.S. Geology Survey (USGS). (2010). Geo Community. Las accessed June 30, 2010, http://data.geocomm.com/

Veve, T.D. and Taggart, B.E. (1996). *Atlas of Ground-Water Resources in Puerto Rico and the U.S. Virgin Islands.* (WRI 94-4198). U.S. Geological Survey: Water Resources Investigations.

Vrijheid M. (2000). Health Effects of Residence near Hazardous Waste Landfill Sites: A Review of Epidemiologic Literature, *Environmental Health Perspective* 108(suppl 1):101-112.

Watkins, D.W., McKinney, D.C., Maidment, D.R. and Lin M. (1996). Use of Geographic Information Systems in Ground-Water Flow Modeling", *Journal of Water Resources Planning and Management*, 122(2), 88-96.

White, W.B. (1999). *Groundwater Flow and Transport in Karst, in The Handbook of Groundwater Engineering*, Boca Raton: CRC.

White, W.B. (2002). Karst Hydrology: Recent Developments and Open Questions, *Engineering Geology*, 65(2-3), 85–10.

Wycisk, P., Weiss, H., Kaschl, A., Heidrich, S., and Sommerwerk, K. (2003). Groundwater pollution and remediation options for multisource contaminated aquifers (Bitterfeld/Wolfen, Germany). *Toxicology Letters*, 140-141, 343- 351.

Zack, A., Rodriguez-Alonso, T. and Romas-Mas, A. (1987). *Puerto Rico Groundwater Quality.* (OFR 87-0749). US Geological Survey.